RESEARCH

UDOT CONNECTING COMMUNITIES

Utah Department of Transportation - Research Division
4501 South 2700 West, Box 148410 - Salt Lake City, Utah 84114-8410

Report No. UT-09.09

FEASIBILITY OF USING HIGH-STRENGTH STEEL AND MMFX REBAR IN BRIDGE DESIGN

Prepared For:

Utah Department of Transportation
Research Division

Submitted By:

Utah State University
Department of Civil & Environmental Engineering

Authored By:

Paul Barr
Kathryn Wixom

July, 2009

THIS PAGE INTENTIALLY LEFT BLANK

DISCLAIMER

The authors alone are responsible for the preparation and accuracy of the information, data, analysis, discussions, recommendations, and conclusions presented herein. The contents do not necessarily reflect the views, opinions, endorsements, or policies of the Utah Department of Transportation and the US Department of Transportation. The Utah Department of Transportation makes no representation or warranty of any kind, and assumes no liability therefore.

Technical Report Documentation Page (FHWA Abstract Page)

1. Project No.	2. Government Accession No.	3. Recipient's Catalog No.
UT-09.09		

4. Title and Subtitle	5. Report Date
FEASIBILITY OF USING HIGH-STRENGTH STEEL AND MMFX REBAR IN BRIDGE DESIGN	July, 2009
	6. Performing Organization Code
7. Author(s)	8. Performing Organization Report No.
Paul J. Barr and Kathryn Wixom	UTCM 09-09
9. Performing Organization Name and Address Utah State University Department of Civil and Environmental Engineering Logan, UT 84322-4110	10. Work Unit No. (TRAIS) 5242501D
	11. Contract or Grant No. 059263
12. Sponsoring Agency Name and Address Utah Department of Transportation 4501 South 2700 West Salt Lake City, Utah 84114-8410	13. Type of Report and Period Covered Final Report 07/07 – 07/09
	14. Sponsoring Agency Code PIC No. NOT SPR Project

15. Supplementary Notes
Prepared in cooperation with the Utah Department of Transportation or U.S. Department of Transportation, Federal Highway Administration

16. Abstract

Pressed by increases in construction costs coupled with insufficient funding for maintenance and new construction, many state and federal agencies are now specifying a service life of 75 years for all concrete bridges without significant repairs. In order to achieve this longer service life, better materials are required. MMFX Microcomposite Steel is a proprietary alloy that the company claims has greater corrosion resistance and structural properties which can achieve a service life of up to 75 years. This report summarizes previous research and UDOTs experience with the use of MMFX Microcomposite Steel as deck reinforcement.

17. Key Word	18. Distribution Statement
MMFX Steel, Deck Reinforcement	

19. Security Classif. (of this report)	20. Security Classif. (of this page)	21. No. of Pages	22. Price
Unclassified	Unclassified	84	n/a

ACKNOWLEDGEMENTS

The authors express sincere appreciation to Daniel Hsiao of the Utah Department of Transportation research division for his guidance throughout the project. We would also like to thank Boyd Wheeler, Tim Beal and Scott Andrus who were part of the technical activity committee.

EXECUTIVE SUMMARY

Pressed by increases in construction costs coupled with insufficient funding for maintenance and new construction, many state and federal agencies are now specifying a service life of 75 years for all concrete bridges without significant repairs. In order to achieve this longer service life, better materials are required. MMFX Microcomposite Steel is a proprietary alloy that the company claims has greater corrosion resistance and structural properties which can achieve a service life of up to 75 years.

Various short-term research projects have been conducted to verify these claims. To date, this research has established the enhanced corrosive resistant properties primarily by short-term tests performed primarily in an aqueous corrosive induced environment or with steel embedded in concrete blocks with little data resulting from actual structures. These enhanced corrosive properties are likely due to the increased levels of alloying elements such as chromium (Cr) content.

The researchers have found that MMFX Microcomposite Steel has a critical chloride concentration that is about 4 times higher than that of carbon steel and cost approximately $.30 more per pound. In addition, when the steel does start to corrode it corrodes at a slower rate than carbon steel. Although these results appear promising and in all likelihood will be validated with long-term tests, at present the long-term data on MMFX Microcomposite Steel is scarce. Some of the major research findings are:

- The research that has been performed thus far on the corrosive properties of MMFX Microscomposite Steel has demonstrated that it has a critical chloride threshold that is approximately four times higher than that of mild reinforcement (not epoxy-coated rebar).
- Researchers have found that the rate of corrosion of MMFX is smaller (between one-third and two-thirds) of mild reinforcement. Some studies have shown that the corrosive rate increases over time.
- Most stainless steel specimens tested performed better than MMFX Microcomposite Steel, but cost more likely due to their higher chromium contents.
- While many of the rapid tests that have been performed for this research do allow for a quick evaluation that can be used to rate different types of steel, they do not provide a reliable correlation between short-term test results and in-situ results that are required to make accurate life-cycle costs.

In an effort to gain experience with the performance of MMFX for an in-service bridge, UDOT replaced the conventional epoxy coated rebar in the US-6/White River Bridge with MMFX Microscomposite Steel. The contractor and employees noted that there was no additional labor associated with the placement of MMFX Steel in comparison to epoxy coated rebar. However, MMFX steel does have a higher initial cost and there is some question in regards to its availability. As such the researchers make the following recommendations.

- For critical concrete bridge decks that are going to be exposed to large amounts of traffic and salting, UDOT should consider using MMFX steel or some other type clad or stainless steel rebar.
- For Concrete bridge decks that are not exposed to large amounts of traffic and salting, UDOT should consider the continued use of epoxy-coated rebar until more personal experience is gained on the pilot bridge or more long-term data is gained from bridges built with MMFX steel in other states.
- UDOT should monitor the corrosion potential of the pilot bridge.
- UDOT should investigate other types of corrosion resistant reinforcement (i.e. Zn/EC bars).
- UDOT should not use different types of steel for the top and bottom mats until more research is performed to insure that cracking does not occur at the bottom of the deck.

TABLE OF CONTENTS

LIST OF FIGURES

LIST OF TABLES

CHAPTER 1 : INTRODUCTION

1.1 MMFX Background

According to a Federal Highway Administration Report (Yunovich et al. 2001) the annual cost of corrosion for highway bridges is estimated to be between $6.43 and $10.15 billion. It is further estimated that it will cost nearly 3.8 billion dollars to replace bridges that have become structurally deficient over the next 10 years, between $1.07 to $2.93 billion for maintenance of concrete bridge decks, between $1.07 to $2.93 billion for superstructures and substructures, and nearly 0.50 billion for maintenance of steel bridges. While these costs are significant, the cost due to traffic delays will be many times higher. Therefore, reducing the cost of corrosion in the nation's highway bridges is a major undertaking that needs to be addressed in order to use scarce state and federal dollars.

In order to mitigate the increasing costs due to corrosion, many state and federal agencies started using epoxy-coated rebar in the mid 1970s. The epoxy coating is applied by spraying a dry powder over cleaned, preheated rebar. This powder, when dried, is intended to provide a tough impermeable coating that would prevent the chloride and moisture from interacting with the rebar. This coated rebar costs approximately 20% more than black steel rebar, but the estimated extended service life obtained with these bars ranges between 5 to 25 years (VTRC 2003). Despite these benefits, there are some draw backs to using epoxy-coated rebar. Epoxy-coated rebar cannot be bent in the field and the bond to the concrete is not as good as regular rebar. It has also been found that epoxy-coated rebar performed better in the superstructure than the substructure. For example, the Florida Department of Transportation noted that premature corrosion had begun after only 6 to 9 years in the substructure of bridges built in some marine environments. Overall however, it is estimated that of the 20,000 bridge decks that have been built since the early 1980s, roughly 95 percent use epoxy coated rebar.

In addition to epoxy-coated rebar, some agencies have tried other means to prolong the service life of their structures. Improvements to the concrete mix design that

result in low chloride-permeable concrete have been developed. Barriers have also been used to impede the chloride in the concrete. Chemical admixtures have been invented that reduce the concretes corrosion potential at specific chloride levels and mineral admixtures such as silica fume are used to make the concrete less permeable. Substituting the black or epoxy-coated rebar with more corrosion resistant rebar made with corrosion-resistant alloys, composites, or clad materials have also been developed. It is estimated; the use of stainless steel rebar for example, can prolong the service life of the bridge to 75 years and up to 120 years in some cases

Despite the apparent benefits of using more corrosion resistant rebar, the initial cost can be prohibitive. For example, the cost of clad rebar and stainless steel rebar is nearly 2 and 4 times more than that of epoxy-coated rebar (VTRC 2003). This higher initial cost has impeded the widespread use of this more corrosion resistant rebar.

Recently, a new product called MMFX Microcomposite Steel has been introduced into the market. The owners of this proprietary alloy claim that MMFX steel is five times more corrosion resistant and three times as strong as conventional rebar. These enhanced properties can lead to lower labor costs, quicker construction time, less amount of reinforcement, and enhanced corrosion resistant properties. In addition to these enhanced properties the cost of MMFX steel is significantly lower than other stainless steel rebar. This literature review focuses on the use of MMFX steel as an improved alternative for bridge deck applications.

1.1.1 Corrosion Process

The corrosion process for a new bridge is shown graphically in Figure 1.

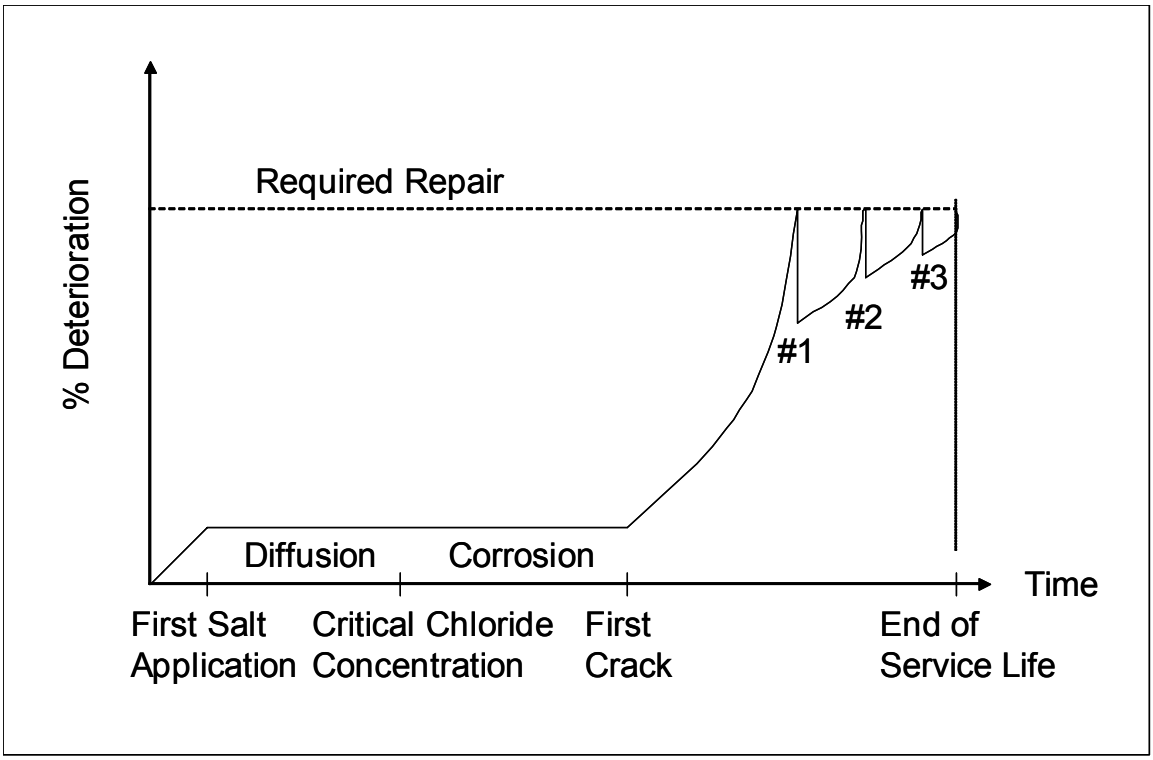

Figure 1-1 Service Life of a Bridge

When a bridge is newly constructed, the concrete cover provides protection to the rebar by acting as a barrier and also helping in creating an alkaline environment. This alkaline environment results in an inert film of ion oxide that covers the rebar and acts to protect the rebar against corrosion.

Eventually, however, after repetitive exposure to deicing salts or marine water the chloride works its way through the concrete and breaks down the film and depassivates the rebar. This process can be minimized by increasing the concrete cover or reducing the diffusion of the chlorides by reducing the deck cracking or making the concrete mix design less permeable. While reducing the permeability of the concrete is a plausible solution, increasing the cover can add excessive dead load to the superstructure and can limit the span capabilities for a given girder size.

Once areas of chloride reach the rebar, an electrical circuit is created within the bridge. The chloride concentrations around the rebar serve as anodes, areas that don't have chloride concentrations serve as cathodes, the rebar as conductors, and the surrounding concrete as the electrolyte. When the chloride concentration around the rebar reaches a critical level, corrosion begins. The advantage of using corrosion resistant rebar is that it has a higher critical chloride threshold in comparison to black rebar likely due to the increase in the percentage of Chromium (Cr).

Once corrosions commences, it's self sustaining. The rust that is formed as a result of the corroding steel occupies three to six times the volume of the original rebar. The stresses that are caused by this expansion in area results in cracks, delaminations, and spalling. Some researchers have found that cracking or spalling will occur when as little as 25 μm (1 mil) of the steel surface corrodes (Pfeifer 2000). This cracking or spalling consequentially facilitates new chlorides to reach the rebar, which in turn increases the rate of corrosion.

1.2 High Performance Steel Background

In 1994, a research program to develop high performance steel (HPS) for bridges was launched by the Federal Highway Administrations (FHWA), the U.S. Navy and the American Iron and Steel Institute (AISI). The purpose of the program was to develop high performance weathering steels with increased toughness and weldability. Because of this initiative grade HPS 50W and grade HPS 70W steels are now commerically available while HPS 100W is still under development (FHWA, 2002).

In 1997, the first high performance steel bridge was opened in Snyder, Nebraska. As of 2002, more than 150 bridges nationwide have used high performance steel in their designs. This number includes the number of bridges that are in service, under construction or in the design phase (Focus 2002). The distribution of these 150 bridges can be seen in Figure 1-1.

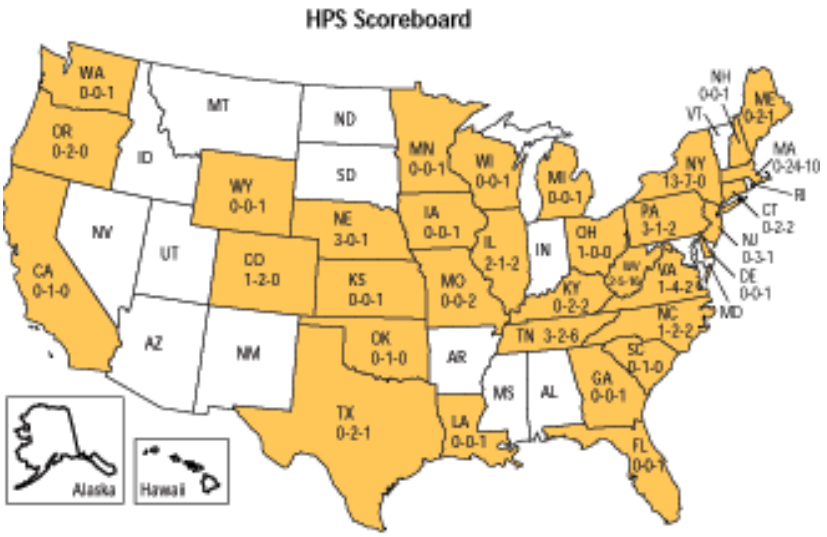

Figure 1-2: Distribution of HPS Bridges in the United States (Focus, 2002)

1.2.1 Advantages & Disadvantages

One of the main goals in the HPS research program was to develop bridge steels with improved weldabilty. In efforts to eliminate hydrogen-cracking, minimum preheat and interpass temperature as designated for welding. Because preheating increases time and costs, the goal was to develop steel that require lower preheat temperatures. The reduction of preheat and interpass temperatures was accomplished and is listed in Table 1-1.

Table 1-1: Minimum Preheat and Interpass Temperature (FHWA, 2002)

Diffusible Hydrogen = H4*

	To ¾"	Over ¾" to 1 ½"	Over 1 ½" to 2 ½"	Over 2 ½"
Grade 70W	50°F (10°C)	125°F (52°C)	175°F (79°C)	225°F (107°C)
HPS 70W	50°F (10°C)	70°F (21°C)	70°F (21°C)	125°F (52°C

There have been many advantages that have come from the use of HPS in bridges. These advantages include the following:

- Reduced number of girder lines
- Reduced weight of bridge
- Shallower girders to help with vertical clearance requirements
- Reduced number of piers on land or obstructions in streams
- Increased span lengths
- Improved weldability
- Higher fracture toughness

The major disadvantage of high performance steel is the increased cost per pound. In 2002, the FHWA determined that the inplace cost of using HPS 70W was 0.15 - 0.25 dollars per pound more than using grade 50W steel. This make HPS 70W approximately 15% more per pound then grade 50W steel.

1.3 High Performance Steel Study

The main objective of this study is to determine when the use HPS is cost beneficial. To determine this, three alternatives will be looked at. The girders that will be used in the three alternatives are composed of the following:

- Homogeneous 50W steel
- Homogeneous HPS 70W steel
- Hybrid- HPS 70W and 50W steel

The hybrid girders will use HPS 70W steel for both flanges and 50W steel for the web. Each design alternative will be designed for span lengths from 50 feet to 200 feet with intermediate bridges designed at 25 foot increments. Single span and two span bridges will be investigated. By comparing the design alternatives, it will be possible to determine the span lengths where using HPS will decrease the girder weight enough to make up for the cost increase of HPS.

1.4 Concrete Deck Design Study

The AASHTO LRFD Specifications give two allowable design methods for a concrete bridge deck. These two methods include the Emperical Method and the Equivalent Strip Method. The Emperical Method is the most common method used by bridge engineers. In addition to the HPS study, this research will also compare the required area of reinforcement according to the two methods at several girder spacings. The girder spacings range from 4 feet to 14 feet. The following deck steel will be compared:

- Transverse Reinforcement for Positive Moment Regions
- Transverse Reinforcement for Negative Moment Regions
- Bottom Layer of Longitudinal Reinforcement

By looking at the required area of steel for the previous three cases we will be able to see how these two methods compare to each other.

1.5 MMFX Study

The last phase of this research will be the actual placement of MMFX steel in a UDOT bridge deck. This implementation phase of the research will be used to determine whether there are any construction issues that are associated with the placement of MMFX steel in comparison to conventional epoxy coated rebar.

CHAPTER 2 : LITERATURE REVIEW

The following chapter summarizes the previous research that was review for this study. The literature reviewed discusses the material properties of MMFX, HPS, case studies, and design comparisons that have been conducted. The included case studies provide information on projects in which MMFX and HPS was used. This information includes lessons learned and advantages seen from using MMFX and HPS in bridges.

2.1 Introduction

Various researchers have investigated the corrosion potential of regular, epoxy-coated and corrosion resistant reinforcing steel. The methods that have employed by these researchers can be broken down into three categories (Hartt 2004):

1. Short-Term Laboratory studies in liquid corrosion conducive environments.
2. Short-Term Laboratory studies with concrete embedded rebar.
3. Long-Term Studies Involving Test yard and Field exposed concrete specimens.

Experiments in category 1 are likely the least expensive and focus on obtaining information such as the ph or the critical chloride concentration. Some of these experiments can be used to rank different types of steel, but do not accurately simulate actual field conditions. Experiments in category 2 replicate field conditions more closely that category 1 and can be used to measure the influence that other parameters such as water-to-cement ratios and concrete cover have on the corrosion of the rebar. These experiments can also determine the time to corrosion in addition to the critical chloride concentration and ph. The costliest but most realistic is data gathered from specimens in category 3. These types of structures are actual structures that have been built as part of a demonstration or other project. The research that has been performed using MMFX in each of these three categories is discussed below.

2.2 Laboratory Studies in Liquid Corrosion Environments

In Section 2.2, research that was associated with the study of corrosion of MMFX in liquid environments is reviewed.

2.2.1 Trejo and Pillai (2003) and Trejo and Pillai (2004)

As part of a research project that was partially funded by MMFX Technologies Corporation a new procedure was developed to experimentally determine the critical chloride concentration levels for ASTM A615, A 706, microcomposite (MMFX), 304 stainless steel, and 316LN stainless steel reinforcements. Preliminary testing by the researchers indicated that the inverse of the polarization resistance (R_p) significantly increased when the reinforcing bar changed from a passive to an active state. The researchers monitored the polarization resistance by embedding the reinforcement in a mortar which had a water:cement:sand ratio of 1:2:4.5. The rate at which the chloride ions penetrated into the mortar was increased by applying a potential gradient across two electrodes. A solution of 3.5% chloride ions were then introduced to the system and the polarization resistance of the steel were monitored.

The researchers found that the mean critical chloride concentration for the microcomposite (MMFX) steel was 4.6 kg/m^3 (7.7 lb/yd^3) based on the unit weight of the mortar. In comparison, the mean critical chloride concentration for the SS 304 and SS316LN stainless steels were 5.0 kg/m^3 (8.5 lb/yd^3) and 10.8 kg/m^3 (18.1 lb/yd^3) respectively. These values were noticeably higher than those measured for the ASTM A 615 (0.5 kg/m^3 (0.9 lb/yd^3) and ASTM A 706 (0.2 kg/m^3 (0.3 lb/yd^3) steels. It should be noted that prior to testing of these specimens, the mill scale had been removed for both the stainless steel specimens, but not for the composite (MMFX) specimens. The researchers commented that the presence of mill scale that is tightly bound may provide a physical barrier, this results in the passive film that forms and protects rebar from corroding may not develop.

2.2.2 Popov et al. (2002)

At the request of MMFX Technology Corporation, the authors performed and experimental study on A615 carbon steel, A706 carbon steel, A615 with mill scale and light corrosion, MMFX with mill scale, MMFX without mill scale, and SS304 and SS316

stainless steel. The testing for all steel was performed in a solution with a pH=12.5 which was meant to simulate the rebar-concrete boundary.

The authors found that the MMFX steel had corrosion rates that were lower than both the A615 and A706 steel. The authors concluded that the MMFX steel forms a stable passive film that helped keep the corrosion rate low. The test results also indicated that in the presence of chloride, the MMFX Steel with mill scale had a lower corrosion rate in comparison to the MMFX Steel without mill scale

2.2.3 Hartt et al. (2004)

The corrosion resistance of various steel specimens was evaluated based on successive immersion and drying cycles in a simulated concrete pore solution for this research. The steel that was monitored for this study included types 316, 2201, 2201P (pickled), and 2205 stainless steels, 316 stainless steel clad rebar, MMFX steel and black bar. In addition to the "as-is" condition of the rebar, the MMFX and clad stainless steel bars were tested in an abraded and surfaced damaged conditions. The abraded condition was created by applying a rotating wire brush to the surface for approximately 30 seconds. The damaged condition was fashioned by drilling a 0.25 in. hole to a depth of 0.125 inches. The depth of this hole was meant to insure that the entire surface of the stainless steel bar was penetrated. The time to corrosion was measured for these experiments by monitoring the polarization resistance of the specimens.

The researchers found that the corrosion rates based on the polarization resistance increased in time for the black bar and MMFX steel where the corrosion rates for the other stainless steel specimens remained relatively constant. The results also indicated that the 316 stainless steel was the best performer and the black bar was the worst. The ranking of the various steels from worst to best was Black steel, MMFX, Type 2201/Type 2201P stainless steel, Type 2205 Stainless Steel, and Type 316 stainless steel. The corrosion rate for the MMFX steel was approximately 30 great than the 316 stainless steel, but still better than the black rebar.

2.3 Laboratory Studies with Concrete Embedded Rebar

In Section 2.3, research associated with the corrosion of MMFX steel embedded concrete is summarized.

2.3.1 Clemena and Virmani (2003)

As part of this research positive machined stainless steel bars (304), stainless-clad carbon steel bars, MMFX bars, bars made with a new "lean" duplex stainless steel (2101 LDX), carbon steel coated bars with a 2-mil layer of arc sprayed Zn and then epoxy coated, two conventional stainless steel (316LN and 2205), and carbon steel bars were tested for their corrosion potential. Each of these bars were embedded in two layers of a block of concrete and sub sequentially subjected to alternating cycles of saturating with a salt solution for three days and drying for four days. As part of the experiment, the researchers investigated the possibility of using mixed types of steel by embedding the less corrosive steel in the top and carbon steel in the bottom for some experiments. The time to corrosion was determined by monitoring their macrocell current, corrosion current and open circuit potential for 2 to 3 years.

Upon the conclusion of the testing, the researchers found that in comparison to the carbon steel bars, the two stainless steel bars (316LN and 2205), the positive machined stainless steel bars (304), and stainless clad carbon bars had a critical chloride threashold that was between 9.8 and 12.4 times larger. The MMFX bars were between 4.7 to 5.9 times larger and the duplex stainless steel (2101) was between 2.7 and 3.4 times larger. Of particular note was that the researchers found that the carbon steel bars that were first sprayed with zinc and sub sequentially coated with epoxy had a chloride threashold that was between 8.0 to 10.1 times larger than the carbon steel.

The corrosion rates also varied for the different bars. The 316LN, 2205, R304 and the clad bars had very low corrosion rates. The zinc-epoxy coated bar had a corrosion rate that was 2 orders of magnitude less than even the stainless steel bars. In contrast, the MMFX and 2101 bars had a high corrosion rate from nearly the start.

The authors also cautioned using different types of reinforcing bars for the top and bottom layers of steel in a bridge deck. While the motivation of using the less

corrosive steel in the top of the deck where the chloride is applied and a less expensive steel like carbon steel in the bottom to save money appears cost effective, the authors found that in certain circumstances the bottom steel can corrode and cause cracking at the bottom of the bridge deck.

2.3.2 Jolley (2003)

MMFX steel, epoxy-coated steel and uncoated mild reinforcement were tested as part of this research at Iowa State University in order to determine whether MMFX steel provides superior corrosion resistance. The specimens were testing in accordance to ASTM G 109 Accelerated Corrosion Testing Program and the Rapid Macrocell Accelerated Corrosion Test. For the ASTM G 109 test, the steel specimens were embedded in concrete blocks that were precracked by inserting a shim either in the longitudinal or transverse direction. The specimens for the Rapid Macrocell Accelerated Corrosion Test are submerged in two canisters. In one canister, a simulated pore solution that contains sodium chloride surrounded the specimen. In the other canister, two specimens were placed in a solution with no chlorides. The specimens from these two canisters are connected by means of a salt bridge and a resistor. All specimens were tested in the "as-is" condition in addition. In addition, some epoxy-coated specimens that had four holes drilled in them that breached the epoxy coating. In addition, some epoxy coated specimens were tested with the epoxy coating chipped of by means of a razor blade.

The researchers did have some variations between redundant specimens. However, the researchers were able to conclude that according to the tests specimens for the ASTM G 109 test only the uncoated mild reinforcement exhibited severe corrosion potential risks. They found that low to intermediate corrosion potential risks were found for all of the remaining steel regardless of the surface condition. For the Rapid Macrocell Test, severe corrosion risks were classified for all types of reinforcement. For this test, the drilled epoxy-coated and uncoated specimens had the greatest potential followed by the epoxy coated bars and MMFX bars had the least corrosion potential.

2.4 Field Exposed Concrete Specimens

While the number of actual structures that have been built using MMFX Microcomposte Steel is growing, the in service, long-term corrosive behavior is still under evaluation and findings are scarce. According to MMFX Technologies Corporation, 24 states have used MMFX Microcomposite Steel in bridge applications. A few examples include a bridge deck fabricated in Iowa where the MMFX Steel was used in the mats for the deck reinforcement. Similar applications have been built in Connecticut, Delaware, Kentucky, Pennsylvania, Texas and Vermont. MMFX steel has also been used in other applications such as the stirrup reinforcement for some precast, prestressed concrete girders that were built in Oklahoma.

In addition to state DOTs using MMFX Steel, some researchers are looking at long-term tests using specimens in the test yard. For example, Hartt et al. (2004) has fabricated concrete slabs that are being exposed to corrosive conditions in the test yard. The results of these test slabs will be compared with those of the shot-term testing when they become available.

2.5 Independent Review of Testing

At the request of MMFX Technologies Corporation, Zia et al. (2003) performed an independent evaluation of the previous research that had been performed on MMFX steel. The independent evaluation was to validate four specific claims that MMFX Technologies Corporation had regarding MMFX Micorcomposite Steel.

The authors agreed that the claim that MMFX Steel exhibits improved corrosion performance was supported by the test results. They agreed that MMFX Steel appears to have a critical chloride level that is four times higher and corrodes at a rate that is between one-third to two-thirds in comparison to regular carbon steel. They did not agree however that enough research has been performed to state that bridges built with MMFX Steel will have longer times between repairs.

The second claim that the higher levels of chrome and low carbon content resulted in improved corrosion resistance was confirmed. However, the claim that the improved performance approaches that of some stainless steels was not confirmed.

The third claim that MMFX steel is an economical alternative to convention steel was confirmed based on data provided for life-cycle costs. The authors did warn however that this claim should be validated with long-term field testing.

It was also concluded that the final claim that MMFX Steel does not have the variability in corrosion performance in comparison to epoxy-coated steel was not supported by the data.

2.6 Review of High Performance Steel Research

In Section 2.6, a review of select research on high-performance steel is summarized.

2.6.1 Barker and Schrage (2000)

In this article, the authors compared the design and costs associated with using High Performance Steel (HPS). To be able to make theses comparisons, six alternative designs were developed for a bridge at a specific site. The six designs included three homogeneous HPS 70W designs, two homogeneous 50W designs, and one hybrid 50W/HPS 70W design. In the hybrid design, HPS was used in both flanges for the negative moment regions and in the bottom flange for the high stress positive moment regions. In all of the designs, 50W steel was used for the stiffeners, diaphragms, and splice connection plates. These alternative designs were compared to a Missouri Department of Transportation (MoDOT) bridge. This bridge was a symmetric 153 feet continuous two-span bridge with a 24 degree skew. The total width was 70 feet- 8 inches and carried four lanes of traffic. The MoDOT design also called for 9 girders spaced at 8 ft on center.

The alternative designs were compared by changing the girder spacings while keeping the span length, skew, and roadway width constant. The varying girder spacings

included the original 9 girders at 8 ft spacing, 8 girders at 9 ft -3 in spacing, and 7 girders at 10 ft 8 in spacing. This approach allowed for a direct comparison of steel weight and costs.

Several trends were documented during the comparison of the six design alternatives. As the girder spacing increases, the number of girders decreases. In addition, though the individual girder weight increases, the total steel weight still decreases. The bridges using HPS were lighter than those using conventional steel. Also, the design alternatives using HPS in the webs required significantly fewer intermediate stiffeners.

The cost of the six alternative designs was also compared. While the HPS designs resulted in a decrease in weight, the cost of HPS is higher than that of conventional steel. The prices used were the projected steel costs of $968/ton for HPS 70W and $842/ton for 50W. The 7-girder hybrid design resulted in the lowest cost with a savings of 21.9% and 14.6% compared respectively to the 9 girder and 7 girder 50W designs. Although the hybrid design showed a significant cost reduction, the homogeneous HPS designs did not.

2.6.2 Ooyen (2002)

This study focused on the replacement of the Springview South Bridge in north central Nebraska. A prestressed concrete girder bridge and a welded plate girder bridge using HPS were both designed to see which bridge would have the lowest cost. The concrete design was a three span, NU2000 prestressed concrete girder bridge. The steel alternative consisted of two end spans and a middle span. The steel bridge used both 50 ksi and HPS 70 ksi steel. The girders in the positive moment regions were completely made of 50 ksi steel. The girders in the negative moment region were hybrid girders that were composed of HPS 70 ksi in the flanges and 50 ksi steel in the web. By using HPS in the flanges, a 28% reduction of steel in the negative moment regions was achieved. Using HPS in the web would cause the plate thickness to decrease, which would require additional stiffeners. Because of this no significant cost savings was seen in using HPS in the web.

The steel girder design was anticipated to be cost-effective to deliver and construct because the steel girders were in segments under 100 ft while the concrete girders were over 150 ft. The steel girders also weighed 62 tons less than the concrete girders. The project was awarded to the steel alternative because it resulted in a 10% lower cost than that of the concrete alternative.

2.6.3 FHWA High Performance Steel Designers Guide (2002)

Research was started in 1994 by the Federal Highway Administration (FWHA), the U.S. Navy, and the American Iron and Steel Institute (AISI) to develop HPS for the use in bridges. The main push for the HPS research program was to develop bridge steels with improved welding qualities, which inturn reduces costs.

Based on this article, delivery time for HPS is approximately 6 – 10 weeks. The price of HPS is also higher than that of conventional steel. In-place costs of HPS 70W in 2002 ranged between $1.18-1.50/lb produced by quenching and tempering and $1.15-1.45/lb made by the thermal-mechanical controlled process. HPS 70W prices range between $.15-.25/lb higher for in-place costs than that of grade 50W steel. The costs are expected to vary from region to region. Prices are also dependent on the complexity of the structure and market conditions.

HPS was also developed with better atmospheric corrosion resistance in comparison to conventional steel. HPS 70W can be produced by quenching and tempering (Q&T) or thermal-mechanical controlled processing (TMCP). The TCMP method can produce plate lengths up to 125 feet while Q&T in limited to lengths of 50 feet. Currently welding of HPS 70W is restricted to submerged arc and shielded metal arc welding. Other welding processes that are commonly used in bridges are being researched and expected to be approved in the future.

HDR Engineering, Inc. and the University of Nebraska-Lincoln performed a HPS cost study. Using the AASHTO LRFD Bridge Design Specifications, 43 different girder designs were looked at. The designs used grade 50W, HPS 70W, and various hybrid combinations. The study found the following trends that are listed below.

1 HPS 70W results in weight and depth savings for all span lengths and girder spacing.

2 Hybrid designs are more economical for all of the spans and girder spacing. The most economical hybrid combination is grade 50 for all webs and positive moment top flanges, with HPS 70W for negative moment top flanges and all bottom flanges.

3 LRFD treats deflection as an optional criterion with different live load configurations. If a deflection limit of L/800 is imposed, deflection may control HPS 70W designs for shallow web depth.

The researchers also found that there are many advantages for using HPS in bridges. These benefits were summarized in the article and include:

- The high strength of HPS allows the designers to use fewer lines of girders to reduce weight and cost, use shallower girders to solve vertical clearance problem, and increase span lengths to reduce the number of piers on land or obstructions in the streams.
- Improved weldability of HPS eliminates hydrogen induced cracking, reduces the cost of fabrication by lower preheat requirement, and improves the quality of weldment by using low hydrogen practices.
- Significantly higher fracture toughness of HPS minimizes brittle and sudden failures of steel bridges in extreme low service temperatures. Higher fracture toughness also means higher cracking tolerance, allowing more time for detecting and repairing cracks before the bridge becomes unsafe.
- Good 'weathering characteristics' of HPS assures long-term performance of unpainted bridges under atmospheric conditions.
- Optimized HPS girders can be attained by using a hybrid combination of HPS 70W in the negative moment top and bottom flanges, and Grade 50W or HPS 50W in other regions.

- Optimized HPS girders have shown to result in lower first cost and are expected to have lower life-cycle cost.

Many designs haven used the benefits of HPS in their project. The researchers found that as of November 2001, 121 HPS bridges were in the design, construction, or service phase. The western states of California, Colorado, North Dakota, Oregon, Washington and Wyoming now have HPS bridges that are under design, construction or in service.

2.6.4 Lane, Munley, Wright, Simon, and Cooper (1998)

In the past, steels with high strengths did not have optimum properties that benifited weldability, toughness, and corrosion resistance. As part of an program to change this state, the Federal Highway Administration launched a high-performance steel initiative to develop a steel that would be cost-effective, safe, and durable.

Steel with strengths less than 355 Mpa have not shown significant problems, therfore the research initiative focused on higher-strength grades. The concerns about corrosion resistance have grown because of the high cost and environmental impact associated with re-painting bridges. Painting bridges was traditionally used to protect bridges from corrosion. Therefore, HPS grades are being developed to have corrosion resistance characteristic greater or equal to that of A588 weathering steel.

Weldability was another characteristic that was looked at for improvement. Welding defects, often caused by undesirable conditions, can add significant costs to bridges. HPS was developed with lower carbon levels which makes the steel more weldable. Improving weldability will make the steels more tolerant of welding procedures and various conditions. The level of quality assurance inspections may also be reduced and the costs associated with inspections will be decreased.

Toughness, the ability of steel to ductilely deform under a load, of HPS was also increased. This characteristic was investigated because of its importance in low temperature conditions. By achieving a steel with high toughness, the steel would be able to handle more fabrication flaws and extreme loading events. The imporved characteristic in HPS, including strength, corrosion resistance, weldability, and

toughness will not only make the initial cost decrease but will also decrease the life-cycle costs and performace of bridges.

2.6.5 Wasserman, Pate, and Huff (2005)

This article summarizes three bridges in Tennessee that were constructed using high performace steel. The first HPS bridge built in Tennesse was the State Route 53 bridge over the Martin Creek embankment. It was designed with two 235.5 foot spans carrying a 28 foot roadway. The girders used HPS 70W steel and the cross-frames used grade 50W. The original design, composed entirly of grade 50W, weighed 675,319 pounds at $1.00 per pound. The alternative design, using HPS 70W girders, weighed 42,746 pounds at $1.18 per pound. The alternative using HPS resulted in a decrease of 24.2% in weight and 10.6% in cost. The HPS design was thus used because of the cost reduction.

The second HPS bridge built by the Tennesse Department of Transportation was the State Route 52 over the Clear Fork River. The bridge was a four span bridge that rose 200 feet above the river. With the limited workspace for the cranes the weights needed to be minimized. HPS helped achieve this. Two spans were made entirely of HPS 70W while the other two spans were hybrid girders. Using the HPS design, the lifting weights were reduced by 30%. The HPS design resulted in more advantages than just cost reduction for Clear Fork River Bridge.

The Clinch River Bridge was the third bridge reviewed which looked at improvements with HPS in Tennessee. The 3-span contiunous welded plate girder bridge is located on State Route 58. Seven girders, spaced at 12-foot, 9-inches on center, support the 88-foot wide deck. The negative moment sections were composed entirely of HPS-70W steel. In the production of the girders, the flanges were quenched and tempered while the web was a HPS-70W Thermal Mechanically Controlled Processed plate (TCMP). This was Tennessee's first oppurtunity in using a fabrication process with HPS that did not require tempering. This made it possible to obtain longer plates, which

in turn reduced the number of required butt splices. The TCMP material was also 4 cents per pound cheaper than that of the quenched and tempered material.

CHAPTER 3 : HIGH PERFORMANCE STEEL

There have been many stated advantages in using high performance steel in bridge designs. These advantages include cost savings, ease of constructability, and shallower cross-sections leading to less clearance issues. Not all bridge designs will benefit from using high performance steel. Three separate bridge designs were compared at various spans to see when high performance steel would be advantageous. The three bridge designs at each span used the following materials for the steel girders:

1. Homogeneous 50W
2. Homogeneous HPS 70W
3. Hybrid HPS 70W/ 50W

The hybrid girder design used 50W steel in the web and HPS 70W steel in the flanges. All designs used 50W steel for all miscellaneous steel. These three designs were compared for spans at 25 feet increments that ranged from 50 to 200 feet. Simply supported and two span continuous bridges where designed for each span length.

For this analysis the AASHTO Load and Resistance Factor Design (LRFD) specifications were used. The STLBRIDGE LRFD software was used for the bridge design. The following sections discuss the procedure, according to the AASHTO LRFD specifications and STLBRIDGE LRFD user's manual, used in this analysis.

3.1 Bridge Description

To compare the various bridges the span lengths were changed while other bridge properties remained the same. The deck was assumed to be made of 4 ksi concrete with a thickness of 7.5 inches including a 0.5-inch integral wearing surface. The bridge deck is supported on a 3-inch haunch. The 41-feet wide deck slab is supported on 5 steel girders spaced at 8 feet on center. The concrete deck is reinforced with number 4 bars at 12 inches on center with a clear distance of 2.5-inches from the top of the deck, and number 4 bars at 10-inches on center with a clear distance of 1 inch from the bottom of the deck. Number 4 bars at 8 inches on center are used for the deck's transverse reinforcement. All reinforcing bars have a yield strength of 60 ksi. The bridges were designed so that they

did not require web stiffeners. A cross-sectional view of the bridge can be seen in Figure 3-1.

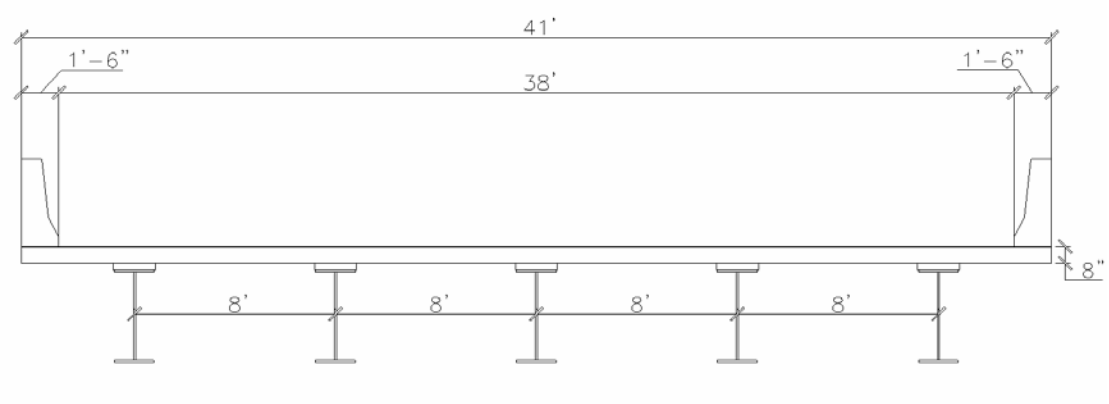

Figure 3-1: Bridge Cross-Section

3.2 Loads

Three types of loads were considered when calculating the structural capacity of the designed bridge. These loading types consist of:

1. Non-composite dead loads
2. Superimposed (long term) dead loads
3. Live loads

Section properties must be determined for each individual load type. The section properties for each loading type are used in the STLBRIDGE LRFD software and described below.

3.2.1 Non-Composite Dead Load

Non-composite dead loads are classified as loads that are applied before the deck is considered composite with the steel girders. These loads include the weight of the steel girders, miscellaneous steel, and the weight of the deck. These loads are applied as a

uniform load over the member. The element moment of inertia is based on the cross section of the steel girder.

3.2.2 Superimposed Dead Load

Superimposed dead loads or long term dead loads are classified as those loads applied after the deck becomes composite with the steel girders. Because these loads are long term, the effects of creep must also be included. To account for creep, according to the AASTHO Specifications, the modular ratio of the steel to concrete is increased by a factor of 3. The element moment of inertia was therefore calculated using the modular ratio of 3n and the effective width of the deck. AASHTO S4.6.2.6.1 lists that the effective width can be taken as the smallest of the following:

1. 1/4 of the span length of the girder
2. Distance to the adjacent girder
3. 12 times the thickness of the deck plus ½ the flange width

The deck was considered composite for the analysis and therefore the moment of inertia was calculated with an uncracked deck analysis.

3.2.3 Live Loads

The moment of inertia for the live load case was calculated similar to that of the superimposed dead loads, but with the modular ratio not multiplied by three. The vehicle live loading on the bridge's roadways was the designated HL-93, which consists of a combination of the following:

- Design truck or design tandem, and
- Design lane load

The AASHTO HS-20 truck (Figure 3-2) was used as the design truck for this analysis.

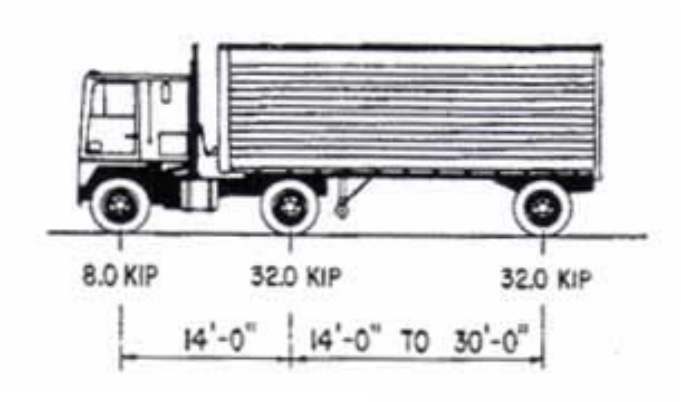

Figure 3-2: Design Truck

The design tandem consists of two 25.0-kip axles with a transverse spacing of 6.0 ft. The lane load consists of a 0.64 klf uniform load equally distributed over the middle 10 feet of the design lane. The design truck shown in Figure 3-2 was also used as the fatigue design truck but with a constant spacing of 30 feet between the 32.0-kip axles, as stated in S3.6.1.4.

Concentrated loads from the design truck and design tandem were used to develop influence lines, which were then used to determine the maximum response. To determine the extreme force effects, the design vehicular live loads are applied according to S3.6.1.3. This section states that the extreme force effects shall be taken as the larger of the following three cases:

1. The effect of the design tandem combined with the effect of the design lane load.
2. The effect of one design truck with the variable axle spacing combined with the effect of the design lane load.
3. For negative moments between points of the non-composite dead load contraflexure and reactions at interior supports, 90 percent of the effect of two design trucks spaced at a minimum of 50 feet between the lead axle of one truck and the rear axle of the other truck, combined with 90 percent of the effect of the design lane load. The distance between the 32 kip axles of each truck shall be taken as 14 feet.

Impact factors, described in S3.6.2, are applied to the truck and tandem loads. The impact factor is applied to the static wheel load to account for dynamic magnification of the moving vehicle's wheel. An impact factor of 1.15 was applied to the fatigue limit state and 1.33 to all other limit states.

3.3 Live Load Distribution Factors

Live load distribution factors help account for the transverse distribution of the live loads. The following formulas used to calculate the distribution factors can be found in S4.6.2.2 of the AASHTO LRFD Specifications. The distribution factors are used along with the impact factors to calculate the values of the design moments and shears due to live loads. The distribution factors can be found by taking the maximum value of the following distribution factors:

- Interior Girder – one design lane loaded
- Interior Girder – two or more design lanes loaded
- Exterior Girder - one design lane loaded
- Exterior Girder – two of more design lanes loaded

The equations used to calculate the distribution of live loads per lane for moment in the interior beam can be found on AASHTO Table 4.6.2.2.2b-1. The moment distribution factor of an interior girder with a single lane loaded can be found using Equation 3-1.

$$DF_{M-si} = 0.06 + \left(\frac{S}{14}\right)^{0.4}\left(\frac{S}{L}\right)^{0.3}\left(\frac{K_g}{12Lt_s^{\,3}}\right)^{0.1} \qquad \textbf{Equation 3-1}$$

where:

$DF_{M\text{-}si}$ = distribution factor for an interior girder with a single lane loaded

t_s = thickness of the deck slab (in.)

S = girder spacing (ft)

L = length of span (ft)

$$K_g = S\left(I_g + A_g e_g{}^2\right) \qquad \textbf{Equation 3-2}$$

where:

I_g = girder moment of inertia (in^4)

A_g = cross-sectional area of girder (in^2)

e_g = girder eccentricity (in.)

The distribution factor of an interior girder with multiple lanes loaded can be calculated using Equation 3-3.

$$DF_{M-mi} = 0.075 + \left(\frac{S}{9.5}\right)^{0.6}\left(\frac{S}{L}\right)^{0.2}\left(\frac{K_g}{12Lt_s{}^3}\right)^{0.1} \qquad \textbf{Equation 3-3}$$

where:

$DF_{M\text{-}mi}$ = distribution factor for an interior girder with multiple lanes loaded

The equations used to calculate the distribution of live loads per lane for moment in the exterior beam can be found on AASHTO Table 4.6.2.2.2d-1. The moment distribution factor of an exterior girder with a single lane loaded can be determined by the lever rule. The lever rule is defined in the AASHTO bridge specifications (2004) as the statical summation of moments about one point to calculate the reaction at a second point. To calculate the moment distribution factor for an exterior single design lane girder, the design truck is placed 2 feet from the barrier. A hinge is then placed at the first interior girder. The moment is calculated about this hinge. Each wheel load is taken as the weight of the axle divided by two. The distribution factor can then be found by multiplying this value by 1.2, the multiple presence factor for a single loaded lane. A graphical representation can be seen in Figure 3-3.

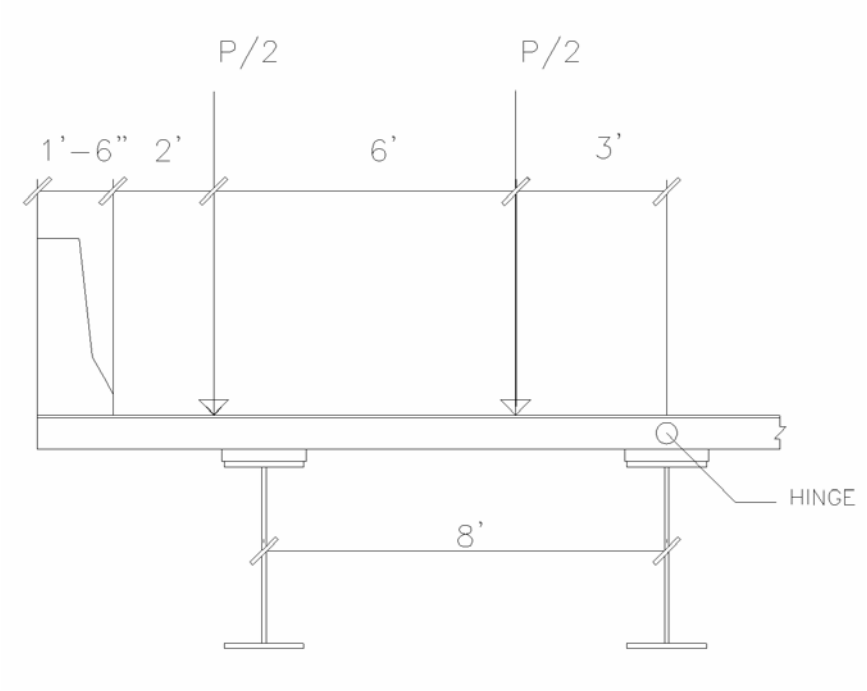

Figure 3-3: Bridge Cross Section Used For Lever Rule

The moment distribution factor for an exterior girder with multiple lanes loaded can be found using Equation 3-4.

$$DF_{M-me} = DF_{M-mi}\left(0.77 + \frac{d_e}{9.1}\right) \qquad \textbf{Equation 3-4}$$

where:

$DF_{M\text{-}me}$ = distribution factor for an exterior girder with multiple lanes loaded

d_e = distance from centerline of exterior girder to inside face of barrier

The moment distribution factor can know be found as the maximum value of the four moment distribution factors calculated using Equations 3-1 through 3-4.

The shear distribution factor must also be found by calculating the distribution factors for the interior girder with single and multiple lanes loaded, and the exterior girder with single and multiple lanes loaded. These distribution factors are described in

AASHTO S4.6.2.2.3. The shear distribution factor for an interior girder with a single loaded lane can be found using Equation 3-5:

$$DF_{V-si} = 0.36 + \frac{S}{25.0} \qquad \textbf{Equation 3-5}$$

where:

$DF_{V\text{-}si}$ = distribution factor for shear on an interior girder with single lane loaded

S = Girder Spacing

The interior girder multiple lane loaded shear distribution can be calculated using Equation 3-6.

$$DF_{V-mi} = 0.2 + \frac{S}{12} - \left(\frac{S}{35}\right)^{2.0} \qquad \textbf{Equation 3-6}$$

where:

$DF_{V\text{-}mi}$ = distribution factor for shear on an interior girder with multiple lanes loaded

The lever rule is also applied when determining the shear distribution factor for the exterior girder with a single loaded lane. This distribution factor will be the same as the moment distribution factor of an exterior girder with a single lane loaded. The lever rule can be seen in Figure 3-3.

Finally, the shear distribution factor for an exterior girder with multiple lanes loaded can be determined using Equation 3-7

$$DF_{V-me} = DF_{V-mi}\left(0.6 + \frac{d_e}{10}\right) \qquad \textbf{Equation 3-7}$$

where:

$DF_{V\text{-}me}$ = distribution factor for an exterior girder with multiple lanes loaded

d_e = distance from centerline of exterior girder to inside face of barrier

The interior and exterior girder shear distribution factors have been calculated and are now compared. The shear distribution factor is then taken as the maximum value of these distribution factors.

3.4 Hybrid Factors

The following reduction factors where applied, as per AASHTO LRFD Section 6.10, to compute the bending section capacities. The hybrid factor is applied in the SLTBRIDGE LRFD program and the following equations and descriptions are taken from the software's user manual. The hybrid factor, R_h, is applied if the stress in either of the flanges due to the factored loads exceed the yield strength of the web. The hybrid factor for composite section in positive flexure can be calculated using the following equation:

$$R_h = 1 - \left[\frac{\beta\psi(1-\rho)^2(3-\psi+\rho\psi)}{6+\beta\psi(3-\psi)} \right] \qquad \textbf{Equation 3-8}$$

where:

$\rho = F_{yw} / F_{yb} \leq 1.0$

$\beta = A_w / A_{fb}$

$\psi = d_n / d$

d_n = distance from the outer fiber of the bottom flange to the neutral axis of the transformed short-term composite section (in.)

F_{yb} = yield strength of the bottom flange (ksi)

F_{yw} = yield strength of the wed (ksi)

A_w = area of the web (in^2)

A_{fb} = area of the bottom flange (in^2)

The hybrid factor for negative flexure is found for two separate cases. The first being when the neutral axis of the hybrid section is located within 10 percent of the web depth from mid depth of the web. If these previous conditions apply the hybrid factor is found using Equation 3-9 from AASHTO S6.10.1.10.1:

$$R_h = \frac{12 + \beta\left(3\rho - \rho^3\right)}{12 + 2\beta} \qquad \textbf{Equation 3-9}$$

where:

$\rho = F_{yw} / f_{fl} \leq 1.0$

$\beta = A_w / A_{tf}$

$\psi = d_n / d$

A_{tf} = for composite sections, total area of both steel flanges and the longitudinal reinforcement included in the section; for non-composite sections, area of both steel flanges (in^2)

f_{fl} = lesser of either the yield strength or the stress due to the factored loading in either flange (ksi)

If the first case does not apply, the following hybrid factor equation is used.

$$R_h = \frac{M_{yr}}{M_y} \qquad \textbf{Equation 3-10}$$

where:

M_{yr} = yield moment for which web yielding is accounted

M_y = yield resistance in terms of moment, when web yielding is disregarded.

3.5 Bending Capacity

The bending capacity of a composite or non-composite section of a steel girder is designed in regions of positive or negative flexure. We will first look at the composite sections in positive flexure. Composite girders are classified as either compact or non-compact sections. As described in the STLBRIGE LRFD manual, compact sections are capable of developing resistance between the yield moment and plastic moment. A non-compact section is limited to a maximum resistance equal to the flange yield strength. A section can be considered compact if it satisfies the following found in AASHTO S6.10.6.2.2:

Fy of the flanges ≤ 70 ksi

$$\frac{D}{t_w} \leq 150 \qquad \textbf{Equation 3-11}$$

$$\frac{2D_{cp}}{t_w} \leq 3.76\sqrt{\frac{E}{f_{yc}}} \qquad \textbf{Equation 3-12}$$

where:

D = depth of the web (in)

t_w = thickness of the web (in)

D_{cp} = depth of the web in compression at the plastic moment (in)

F_{yc} = flange yield stress (ksi)

If the composite section in positive flexure is determined to be compact, then the section can develop a capacity above the yield moment. At the strength limit state, the section must satisfy Equation 3-13 found in AASHTO S6.10.7.1.1.

$$M_u + \frac{1}{3} f_t S_{st} \leq \phi_f M_n \qquad \textbf{Equation 3-13}$$

where:

φ_f = flexural resistance factor (1.0)

M_n = nominal flexural resistance

M_u = factored bending moment about major axis

f_t = flange lateral bending stress in the bottom flange

S_{xt} = elastic section modulus about the major axis to the tension flange M_{yt}/F_{yt}

The nominal resistance of the compact section, M_n, can be found according to AASHTO S6.10.7.1.2. The nominal flexural resistance shall be taken as:

If $D_p \leq 0.1\ D_t$, then:

$$Mn = Mp \qquad \textbf{Equation 3-14}$$

Otherwise:

$$M_n = M_p\left(1.07 - 0.7\frac{D_p}{D_t}\right) \qquad \textbf{Equation 3-15}$$

where:

D_p = distance from the top of the concrete deck to the neutral axis of the composite section at the plastic moment (in.)

D_t = total depth of the composite section (in.)

M_p = plastic moment of the composite section (k-in)

If the bridge is continuous, the nominal flexural resistance shall not exceed the following:

$$M_n = 1.3R_hM_y \qquad \textbf{Equation 3-16}$$

where:

M_y = yield moment (k-in)

R_h = hybrid factor

If the composite positive moment section does not meet the compact section requirements then it is considered non-compact. If the section is non-compact, the tension flange must satisfy Equation 3-17.

$$f_{bu} + \frac{1}{3}f_l \le \phi_f F_n \qquad \textbf{Equation 3-17}$$

where:

$F_{nt} = R_hF_{yt}$ = nominal flexural resistance of the tension flange

f_{bu} = factored bending stress about the major axis

f_l = flange lateral bending stress in the bottom flange

The compression flange shall satisfy:

$$f_{bu} = \phi_f F_{nc} \qquad \textbf{Equation 3-18}$$

where:

$F_{nc} = R_bR_hF_{yc}$ - nominal flexural resistance of the compression flange

3.6 Analysis

Three separate bridge designs were compared at various spans to see when using high performance steel would be advantageous. The three bridge designs used the following materials for the steel girders:

1. Homogeneous 50W
2. Homogeneous HPS 70W
3. Hybrid HPS 70W/ 50W

The hybrid steel girder used a combination of grade 50W steel for all webs and HPS 70W in the top and bottom flanges. This combination was used based on research done by HDR Engineering and the University of Nebraska-Lincoln and past HPS bridge designs have shown it to be cost beneficial.

The bridges were designed using the AASHTO LRFD Specification (2004) and STL BRIDGE LRFD software. The STL BRIDGE LRFD program was chosen because of its capabilities to use hybrid girders in the bridge design. The study conducted looked at cost savings by the weight of the steel girders and did not look into other possible advantages of HPS. When designing the steel girders, W-sections were used for the homogeneous 50W and homogenous HPS 70W designs until they were not suitable for the bridge design. Plate girders were then used when the W-sections available were not large enough to withstand the loads. Plate girders were used in all hybrid girder designs. Also, the bridges were designed so that web stiffeners were not required.

3.6.1 Single Span Bridge

A single span bridge was looked at first. The cross-section for the design bridge can be seen in Figure 3-1. The investigated bridges varied from spans of 50 feet to 200 feet by increments of 25 feet. The weight of a single steel girder designed for a given span can be seen in Figure 3-4. Five steel girders were used in the design of the bridge and therefore the weight shown in the figure can be multiplied by five to achieve the total

steel girder weight. From this figure, the weight per girder for the three designs can also be compared.

W-sections were used in spans ranging from 50 feet to 125 feet for the bridges designed with homogeneous 50W and homogenous HPS 70W steel girders. After spans of 125-feet all designs used plate girders. Plate girders provide more sizing options than are possible when using w-sections. More girder options with size can help achieve a lighter girder weight. Deflection was the controlling mechanism for many of the bridges designed. When using hybrid girders, deflection began to control at a span length of 75-feet. Deflection began to control the HPS 70W design when the span reached 100-feet. The conventional, 50W steel design, deflection did not begin to control the girder design until the span length reached 200-ft.

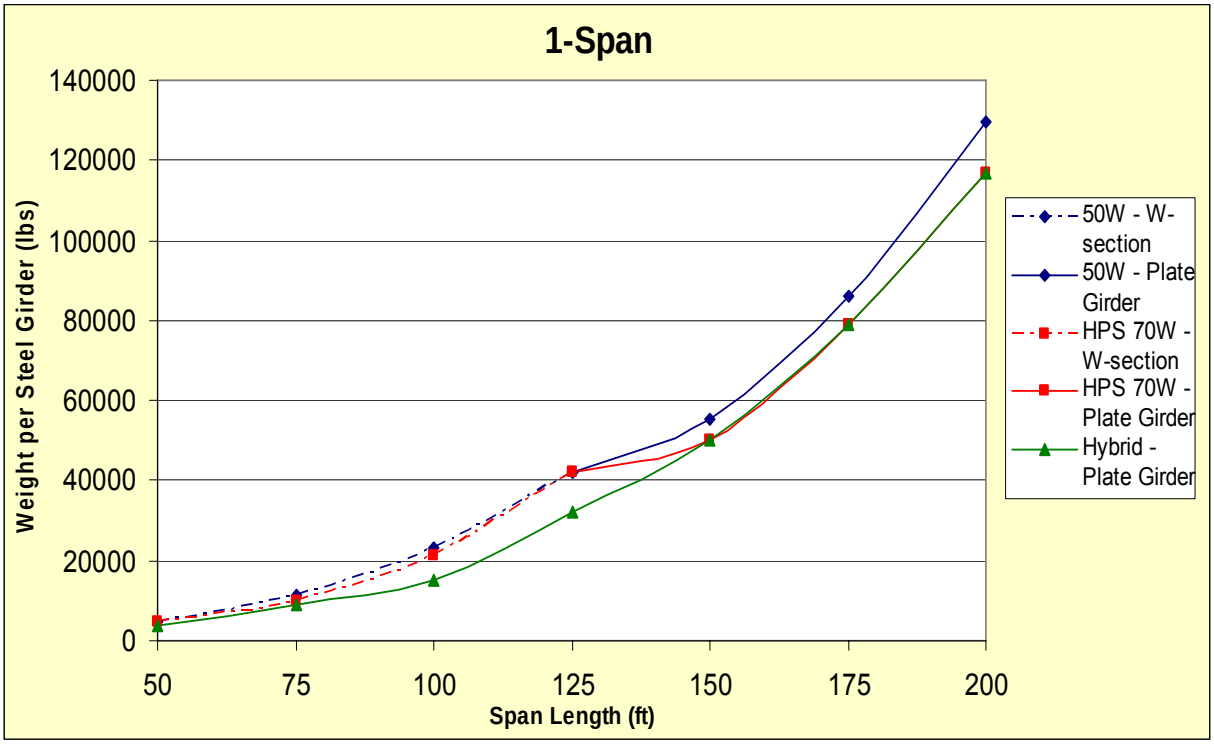

Figure 3-4: Girder Weight per Designed Span Length for a Single Span Bridge

The comparison of the hybrid and homogeneous HPS 70W designs is broken up into spans up to 125-feet and spans larger than 125-feet. For span lengths up to 125-feet,

it can be seen in Figure 3-4 that the hybrid design requires a smaller girder than that of the HPS 70W design. This result is due to the use of plate girders for the hybrid design and W-sections for the homogeneous HPS 70W design. When the span length is larger than 125-feet, both designs yield the same girder size because deflection is the controlling mechanism and therefore the advantages of HPS cannot fully be seen.

By comparing the hybrid and homogeneous HPS 70W designs to the 50W girder design, the largest girder weight difference can be seen at a span length of 100-ft. At this span length the hybrid girder design resulted in a 34% weight reduction compared to the 50W design. For girder spans greater than 125-feet, the girders in the design using HPS weighed on an average of 9 percent less then the design using homogeneous 50W steel. A weight used in Figure 3-4 along with the failure mode and weight decrease for each span length can be seen in Appendix A.

Although the weight of steel of the bridge may be reduced by using HPS, the cost may still increase. According to the FHWA, in 2002 the in-place cost of HPS 70W steel is approximately 0.15 – 0.25 dollars per pound higher than 50W steel. The increased costs that may be associated with using plate girders instead of W-section and also increased costs of welding HPS were not looked at. The decrease in steel weight must be large enough to make up for the increase in price for HPS to be cost-beneficial. Figure 3-5 shows the costs of the three alternatives for the designed span lengths.

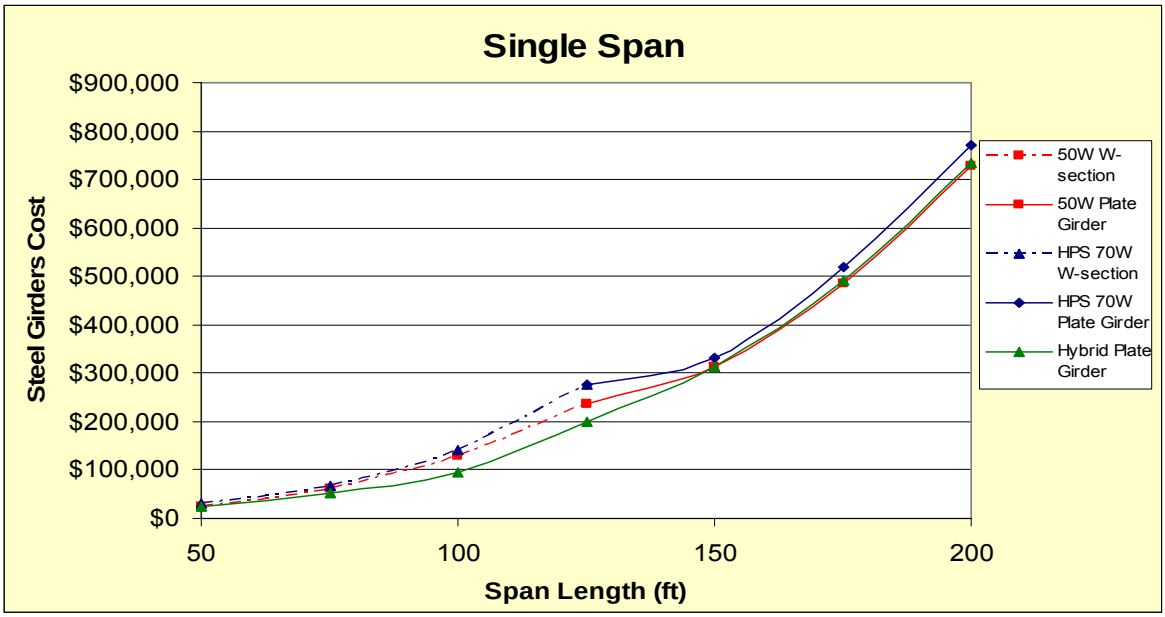

Figure 3-5: Steel Cost per Design Span for a Single Span Bridge

The costs shown in this Figure 3.5 is for all 5 girders. The in-place cost per pound for the steel was taken as average of the costs given in the FHWA High Performance Steel Designers' Guide (2002). The costs used were $1.125 for grade 50W steel and $1.32 for HPS 70W steel.

The cost comparison shows that even though the total steel weight was reduced for spans over 150 feet by using HPS, the cost was still greater than that of the homogeneous 50W design for all span lengths. The hybrid design was found to be the most cost-effective design for span length up to 125-feet, with a maximum price reduction of $36,229 at a span length of 125-feet. For all span length larger than 125-feet the homogeneous 50W steel design was the most cost-beneficial. The costs and the increase/decrease in price of the HPS designs compared to the 50W design can be seen in Appendix A.

3.6.2 Two Span Bridge

Bridges with two continuous spans were also investigated. The cross-section used in the design of the two span bridges is the same as that of the single span bridges. This cross-section can be seen in Figure 3-1. The two-span bridges were also designed for spans of 50-feet to 200-feet. The span length indicated refers to the length of each span, therefore a span length of 50-feet refers to a 100-foot bridge with two 50-foot spans. The weight of a single steel girder for each span can be seen in Figure 3-6. Five steel girders were also used for the two span bridges and therefore the weight shown can be multiplied by five, (girders) and then by two, (spans) to calculate the total steel girder weight of the bridge.

W-sections were used for the homogeneous 50W and homogeneous HPS70W designs for span lengths up to 100-feet. For spans greater than 100-feet, plate girders were used because the available W-sections were not adequate for the design. Because of the use of the W-sections, the hybrid girder design used less steel than the homogeneous HPS 70W steel design for spans of 100-feet and less. For spans greater than 100-feet, the HPS 70W achieved lower weights than that of the hybrid girders because of the ability to reduce the size of the web and still satisfy structural requirements. For these larger spans, the HPS 70W design only was found to only reduce the hybrid design's steel weight by approximately 2 percent.

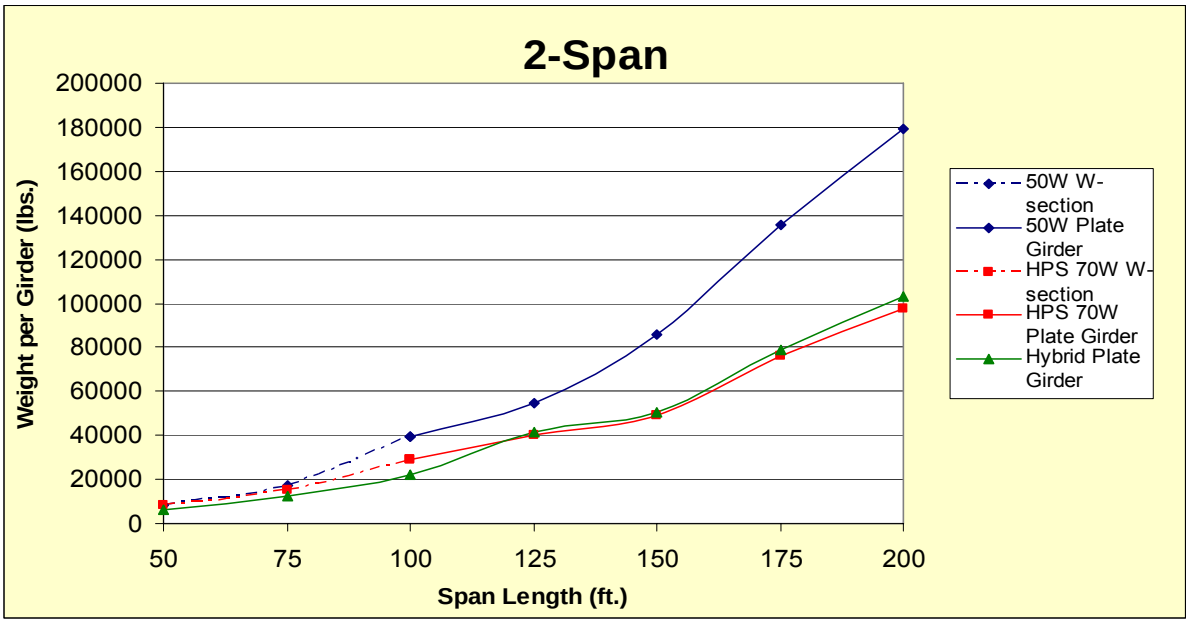

Figure 3-6: Girder Weight per Designed Span Length for a Two Span Bridge

The Strength I limit state controlled in all of the two span bridge designs. Because deflection was not the controlling mechanism, the use of HPS resulted in large reductions of girder weight. For span lengths of 150-feet and greater, the weight of the girder designed with 50W steel was reduced by both the homogeneous HPS 70W and hybrid design by a minimum of 40 percent. The design girder weights, weight reduction, and failure controlling mechanism for each individual design span can be seen in Appendix A. The STL BRIDGE LRFD output used to design the bridges for this study can also be seen in Appendix B. This output includes the moment and shear diagrams, analysis output, stress output, and shear output.

The in-place cost of the steel girders for the two span bridges was also compared. The costs of the alternatives can be seen in Figure 3-7. These costs reflect the price of the five of the girders for both of the span lengths.

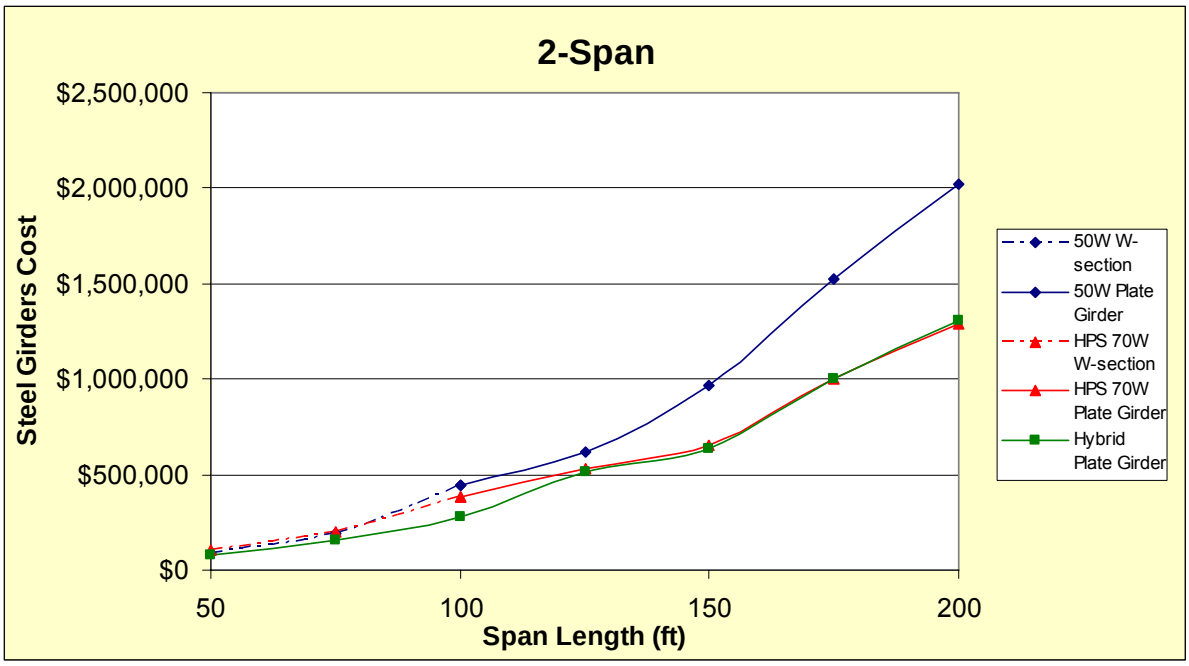

Figure 3-7: Steel Cost per Design Span for a Two Span Bridge

Using HPS in two-span bridges significantly reduced the steel weight for many of the designed span lengths. This large weight reduction caused the cost to also decrease. As shown in Figure 3-7, the hybrid design lead to a decrease in cost, compared to the 50W design, for all span lengths. The largest cost reduction percentage was for the span length of 100-feet which had a 37% cost reduction. The hybrid design for the 200-foot two-span bridge had a price reduction of $708,000. The hybrid design was found to be the most cost-beneficial for all but one span length. For 200-foot span length bridge, the homogeneous HPS 70W design reduced the steel cost by $726,517 which was $18,000 less then the hybrid design. A detailed summary of the cost for the designed bridges can be seen in Appendix A.

CHAPTER 4 : CONCRETE DECK DESIGN

The AASHTO- LRFD Bridge Design Specifications (2004) describe two separate deck design methods. The first is known as the Empirical Design Method. The second is the Approximate Method of analysis, which is also known as the Equivalent Strip Method. The two design methods yield different values for the required deck reinforcement. A comparison of these two methods, provided in this chapter, will show how the two methods differ as a function of the bridge's span length.

4.1 Deck Design

The two deck design methods were compared by varying the number of steel girders and their spacing. To more accurately compare the design methodologies, other deck properties and dimensions remained constant. The concrete deck reinforcement had a top cover of 2 ½ inches, including the ½ inch integral wearing surface, and a 1-inch bottom cover. Each overhang supports an 18 inch wide concrete barrier. The cross-section of the bridge used can be seen in Figure 4-1. The properties of the materials used for the design are as follows:

Reinforcement yield strength = 60 ksi

Girder yield strength = 50 ksi

Concrete deck compressive strength = 4 ksi

Concrete density = 150 pcf

Future wearing surface density = 30 psf

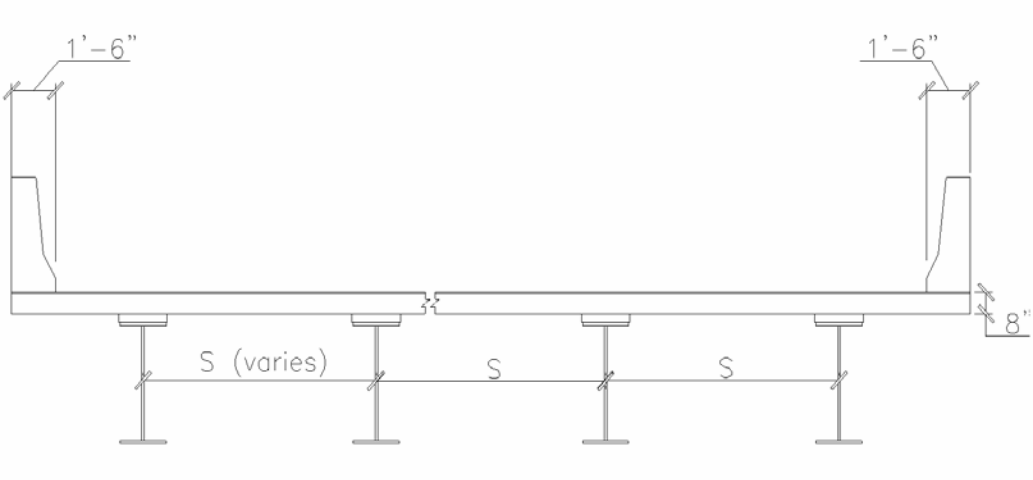

Figure 4-1 : Bridge cross-section for deck design

4.2 Deck Thickness

According to AASHTO Specifications 9.7.1.1, the deck thickness must be greater than 7 inches. This thickness requirement applies to both design methods. While the specifications require a minimum thickness of 7-inches, most jurisdictions require a deck thickness of 8-inches, which includes the ½ inch integral wearing surface. Therefore, an 8-inch deck thickness (including a ½ inch integral wearing surface) was used for the deck design to satisfy the thickness requirement. A deck thickness of 8-inches was used in the self-weight calculations in which the integral wearing surface is considered to participate. In the structural resistance calculations, a deck thickness of 7.5-inches was used and the integral wearing surface was not assumed to participate.

4.3 Equivalent Strip Method

The Equivalent Strip Method is described in Section 4.6.2 of the AASHTO Design Specifications. In this method the deck is divided up into strips perpendicular to the supports. As stated in the Prestressed Concrete Bridge Design Example, the equivalent strip method is based on the following seven steps:

1 A transverse strip of the deck is assumed to support the truck axle loads.

2 The strip is assumed to be supported on rigid supports at the center of the girders. The width of the strip for different load effects is determined using the equations in Figure 4-3.

3 The truck axle loads are moved laterally to produce the moment envelopes. Multiple presence factors and the dynamic load allowance are included. The total moment is divided by the strip distribution width to determine the live load per unit width.

4 The loads transmitted to the bridge deck during vehicular collision with the railing system are determined.

5 Design factored moments are then determined using the appropriate load factors for different limit states.

6 The reinforcement is designed to resist the applied loads using conventional principles of reinforced concrete design.

7 Shear and fatigue of the reinforcement need not be investigated.

The steps in the Prestressed Concrete Bridge Design example, using the Equivalent Strip Method, were followed and are described in the following sections.

4.3.1 Dead Load Moments

Rigid supports were assumed at web centerlines when the moments for the deck transverse strips were calculated. The load factors for permanent loads can be found in AASHTO S3.4.1-2, which can be seen in Figure 4-2. The maximum load factors used for the slab and parapet, and integral wearing surface were 1.25 and 1.5 respectively. The maximum load factors were used in lieu of other loading conditions because they control in deck slab design.

Table 3.4.1-2 Load Factors for Permanent Loads, γ_p.

Type of Load	Load Factor	
	Maximum	Minimum
DC: Component and Attachments	1.25	0.90
DD: Downdrag	1.80	0.45
DW: Wearing Surfaces and Utilities	1.50	0.65
EH: Horizontal Earth Pressure		
• Active	1.50	0.90
• At-Rest	1.35	0.90
EL: Locked-in Erection Stresses	1.00	1.00
EV: Vertical Earth Pressure		
• Overall Stability	1.00	N/A
• Retaining Walls and Abutments	1.35	1.00
• Rigid Buried Structure	1.30	0.90
• Rigid Frames	1.35	0.90
• Flexible Buried Structures other than Metal Box Culverts	1.95	0.90
• Flexible Metal Box Culverts	1.50	0.90
ES: Earth Surcharge	1.50	0.75

Figure 4-2: Load Factors for Permanent Loads

The deck load is comprised of live and dead loads. In comparison, the moment caused by the dead loads constitute a small portion of the total deck load. Because of this, a simplified method is often used and results in negligible differences. The deck dead load moments for a unit width strip can be calculated using Equation 4-1:

$$M = \frac{wl^2}{c} \qquad \textbf{Equation 4-1}$$

where:

M = positive or negative deck dead load moment in the deck for a unit width strip (k-ft/ft)

w = distributed dead load per unit area of the deck (ksf)

l = girder spacing (ft)

c = constant, typically 10 or 12

For this study, C was taken as a conservative value of 10 when the moments due to self weight of the deck and the integral wearing surface were calculated.

4.3.2 Live Load Moments

The live load moments may be estimated by modeling the deck as a beam supported on the girders. The truck live load can be represented by placing one or more axles side by side on the deck or transversely across the deck to maximize the moment. After the wheel loads are positioned the live load moment per unit strip width must then be determined. This can be calculated by dividing the total live load moment by a strip width. The strip width used in the equivalent strip method can be found using the appropriate equation from Table in AASHTO S4.6.2.1.3-1. This table for steel and concrete decks can be seen in Figure 4-3.

TYPE OF DECK	DIRECTION OF PRIMARY STRIP RELATIVE TO TRAFFIC	WIDTH OF PRIMARY STRIP (in.)
Concrete:		
• Cast-in-place	Overhang	$45.0 + 10.0X$
	Either Parallel or Perpendicular	$+M$: $26.0 + 6.6S$ $-M$: $48.0 + 3.0S$
• Cast-in-place with stay-in-place concrete formwork	Either Parallel or Perpendicular	$+M$: $26.0 + 6.6S$ $-M$: $48.0 + 3.0S$
• Precast, post-tensioned	Either Parallel or Perpendicular	$+M$: $26.0 + 6.6S$ $-M$: $48.0 + 3.0S$
Steel:		
• Open grid	Main Bars	$1.25P + 4.0S_b$
• Filled or partially filled grid	Main Bars	Article 4.6.2.1.8 applies
• Unfilled, composite grids	Main Bars	Article 4.6.2.1.8 applies

Figure 4-3: Equivalent Strips

In determining the live load effects the following must be used:

Minimum distance from center of wheel to the inside face of parapet = 1 ft (S3.6.1.3)

Minimum distance between the wheels of two adjacent trucks = 4 ft

Dynamic load allowance = 33% (S3.6.2.1)

Load factor (Strength I) = 1.75 (S3.4.1)

Multiple presence factor (S3.6.1.1.2):

Single lane = 1.20

Two lanes = 1.00

Three lanes = 0.85

Resistance factors:

0.9 strength limit states (S5.5.4.2)

1.0 extreme limit states (S1.3.2.1)

The code also allows for the use of an alternative procedure for determining live load effects. This alternative procedure was used in this analysis. Positive and negative moments per unit width for this method can be determined using AASHTO Table SA4.1-1. A portion of this table can be seen in Figure 4-4. The moments are a function of the girder spacing and the distance from the design section to the centerline of the girders for negative moments. If the designed girder spacing is not available in the table, interpolation may be used.

S	Positive Moment	NEGATIVE MOMENT						
		Distance from CL of Girder to Design Section for Negative Moment						
		0.0 in.	3 in.	6 in.	9 in.	12 in.	18 in.	24 in.
4' -0"	4.68	2.68	2.07	1.74	1.60	1.50	1.34	1.25
4' -3"	4.66	2.73	2.25	1.95	1.74	1.57	1.33	1.20
4' -6"	4.63	3.00	2.58	2.19	1.90	1.65	1.32	1.18
4' -9"	4.64	3.38	2.90	2.43	2.07	1.74	1.29	1.20
5' -0"	4.65	3.74	3.20	2.66	2.24	1.83	1.26	1.12
5' -3"	4.67	4.06	3.47	2.89	2.41	1.95	1.28	0.98
5' -6"	4.71	4.36	3.73	3.11	2.58	2.07	1.30	0.99
5' -9"	4.77	4.63	3.97	3.31	2.73	2.19	1.32	1.02
6' -0"	4.83	4.88	4.19	3.50	2.88	2.31	1.39	1.07
6' -3"	4.91	5.10	4.39	3.68	3.02	2.42	1.45	1.13
6' -6"	5.00	5.31	4.57	3.84	3.15	2.53	1.50	1.20
6' -9"	5.10	5.50	4.74	3.99	3.27	2.64	1.58	1.28
7' -0"	5.21	5.98	5.17	4.36	3.56	2.84	1.63	1.37

Figure 4-4: Maximum Live Load Moments per Unit Width

4.3.3 Design for Positive Deck Moment

The maximum positive moment is used to determine the deck reinforcement. For interior bays, the maximum positive moment occurs close to the center of the bay. Conservatively, the same reinforcement is typically used in all of the deck bays. The maximum unfactored positive live load moment per unit length can be found from AASHTO Table SA4.1-1. The dead load moments caused by the deck weight and future wearing surface were previously described in section 4.3.2. The appropriate load factors were then applied to the moments. The sum of the dead load and live load moments were then used in solving for the required area of reinforcement. The area of reinforcement can be found using Equations 4-2 through 4-4.

$$k' = \frac{M_u}{\varphi b d^2} \qquad \textbf{Equation 4-2}$$

$$\rho = 0.85\left(\frac{f'_c}{f_y}\right)\left[1.0 - \sqrt{1.0 - \frac{2k'}{0.85 f'_c}}\right] \qquad \textbf{Equation 4-3}$$

$$A_s = \rho d_e \qquad \textbf{Equation 4-4}$$

where:

ρ = reinforcement ratio

A_s = required area of reinforcement

M_u = factored dead load and live load moment

Φ = resistance factor for flexure, = 0.9 (S5.5.4.2.1)

d_e = distance from compression face to centroid of tension reinforcement (in.)

The value of b is taken as 12 inches to yield a required area of reinforcement per unit width.

4.3.3.a Check maximum and minimum requirements

After the required area of deck steel is calculated, the minimum and maximum reinforcement requirements must then be checked. The Prestressed Concrete Bridge Design example says that past experience shows the minimum reinforcement requirement, presented in AASHTO S5.7.3.3.2, never controls the deck slab design. The maximum reinforcement requirements can be checked with the equation found in AASHTO S5.7.3.3.1. This standard states that reinforced concrete is over reinforcement if Equation 4-5 is satisfied.

$$c / d_e \geq 0.42 \qquad \textbf{Equation 4-5}$$

where:

d_e = effective depth from the compression fiber to the centroid of the tensile force in the tensile reinforcement (in).

4.3.4 Crack Control for Live Load Positive Moment Reinforcement

The selected positive reinforcement must meet the minimum required amount to maintain crack control. The first step is to determine the allowable reinforcement service load stress for crack control using Equation 4-6.

$$f_{sa} = \frac{Z}{(d_c A)^{\frac{1}{3}}} \leq 0.6 f_y$$ **Equation 4-6**

where:

f_{sa} = reinforced service load stress for crack control

d_c = thickness of concrete cover measured from extreme tension fiber to center of closest bar (in.)

A = area of concrete having the same centroid as the principal tensile reinforcement and bounded by the surfaces of the cross-section and a straight line parallel to the neutral axis, divided by the number of bars (in^2)

Z = crack control parameter (k/in)

Severe exposure conditions were assumed for the analysis and therefore 130 k/in. was used for the control parameter, Z.

The stress in the steel must be calculated and compared to the allowable service load stress calculated in Equation 4-6. As described in the Prestressed Concrete Bridge Design Example, the transformed moment of inertia is calculated assuming elastic behavior. The first moment area of the transformed steel on the tension side about the neutral axis is assumed equal to that of the concrete in compression. After determining the transformed moment of inertia, the stress of the steel can be determined using Equation 4-7.

$$f_s = \left(\frac{Mc}{I}\right) n$$ **Equation 4-7**

where:

f_s = stress in the steel

M = moment acting on a width equal to the reinforcement spacing

I = transformed moment of inertia

n = modular ratio (S6.10.3.1.1b)

c = distance between the neutral axis and the tension face (in.)

The calculated stress in the steel, (Equation 4-7), must be less than that of the calculated allowable service load stress, (Equation 4-6), for the design to be acceptable.

4.3.5 Distance from Center of Grid Line to the Design Section for Negative Moments

As stated in AASHTO S4.6.2.1.6, the design section for negative moments and shear forces for steel beams may be taken as one-quarter the flange width from the centerline of support.

4.3.6 Design for Negative Moment

The unfactored live load negative moment per unit width of the deck can be found on AASHTO Table SA4.1-1, (Figure 4-4). It is based on the girder spacing and the distance from centerline of girder to the design section for negative moment, which was found in the previous section. The appropriate load factor for strength design can then be applied to give the maximum live load factored negative moment. The maximum dead load moments are the same as those used in the design for positive moment. Equations 4-2 through 4-4 are used to calculate the required area of reinforcement for the negative moment region. These design equations are the same as those used to calculate the required area of reinforcement for the positive moment region.

4.3.7 Crack Control for Live Load Negative Moment Reinforcement

The negative moment reinforcement must also meet the minimum required amount to maintain crack control. The equations used to check this requirement are the same as those for the positive moment reinforcement (Equations 4.6, 4.7).

4.3.8 Longitudinal Reinforcement

The longitudinal requirements are different for the top and bottom layer. These requirements are broken up in the following sections.

4.3.8.a Bottom Longitudinal Reinforcement

The bottom distribution reinforcement is presented in S9.7.3.2. The longitudinal reinforcement can be calculated as a percentage of the transverse reinforcement. It states that the percentage of longitudinal reinforcement is calculated using Equation 4-8.

$$\text{Percentage of longitudinal reinforcement} = \frac{220}{\sqrt{S}} \leq 67\% \qquad \textbf{Equation 4-8}$$

where:

S = the effective span length taken as equal to the effective length specified in S9.7.2.3 (ft.); the distance between sections for negative moment sections at the ends of one deck span.

4.3.8.b Top Longitudinal Reinforcement

The code does not have specific requirements to determine the top longitudinal reinforcement. The Prestressed Concrete Bridge Example explains that many jurisdictions use #4 bars at 12 in. spacing for the top longitudinal reinforcement.

4.3.9 Shrinkage and Temperature Reinforcement

Reinforcement that is near the surface of concrete that is exposed to daily temperature changes must be designed for shrinkage and temperature stresses. To ensure that the total reinforcement on exposed surfaces is adequate for temperature and shrinkage stresses, the following check found in S5.10.8.2-1 must be made.

$$A_s \geq 0.11\frac{A_g}{f_y} \qquad \textbf{Equation 4-9}$$

where:

A_g = gross area of the section (in^2)

f_y = yield stress of the deck reinforcement (ksi)

Because the area of required reinforcement is for both the transverse and longitudinal top steel, the total area of steel (A_s) should be divided by two to yield the area of reinforcement per direction.

4.4 Empirical Design Method

The Empirical Design Method can be found in Section 9.7.2 of the AASHTO Specifications. This method is based upon laboratory tests of deck slabs. Four layers of isotropic steel are required for the empirically designed slabs. The reinforcement layers are to be placed as close to the concrete's outside edges as permitted by cover requirements. The reinforcement requirements are listed in Section 9.7.2.5. These requirements state that the minimum amount of reinforcement is as follows:

- 0.27 in^2/ft. for each bottom layer
- 0.18 in^2/ft. for each top layer

The reinforcing steel must have a yield strength of 60 ksi or higher. The reinforcement spacing must be less than 18 inches. There are no additional calculations required for the interior deck reinforcement.

4.5 Analysis

The Equivalent Strip Method and Empirical Method can both be used to calculate a required amount of steel used in a concrete bridge deck. These two methods were compared by calculating the required reinforcement by both methods for eleven different bridges. To be able to compare the methods, the girder spacing was varied while all other dimensions remained constant. The girder spacing for the design bridges varied from 4-feet to 14-feet by 1-foot increments. The required area of steel was compared for the following three categories:

- Transverse reinforcement for the positive moment region
- Transverse reinforcement for the negative moment region
- Bottom layer of longitudinal reinforcement

The first type of reinforcement that was looked at was the transverse reinforcement for the positive moment regions. This required area of reinforcement for both methods was calculated as described previously in this chapter. As the girder spacing increased, so did the area of reinforcement calculated by the equivalent strip method. The area of reinforcement calculated by the empirical method does not depend on the girder spacing, and is therefore the same for all girder spacings. The area of reinforcement using the equivalent strip method is less than that determined by the empirical method up to girder spacings of approximately 9-feet. When the girder spacing is larger than 9-feet, the empirical method yields a smaller required area of reinforcement for the transverse steel in the positive moment region. This trend can be seen in Figure 4-5.

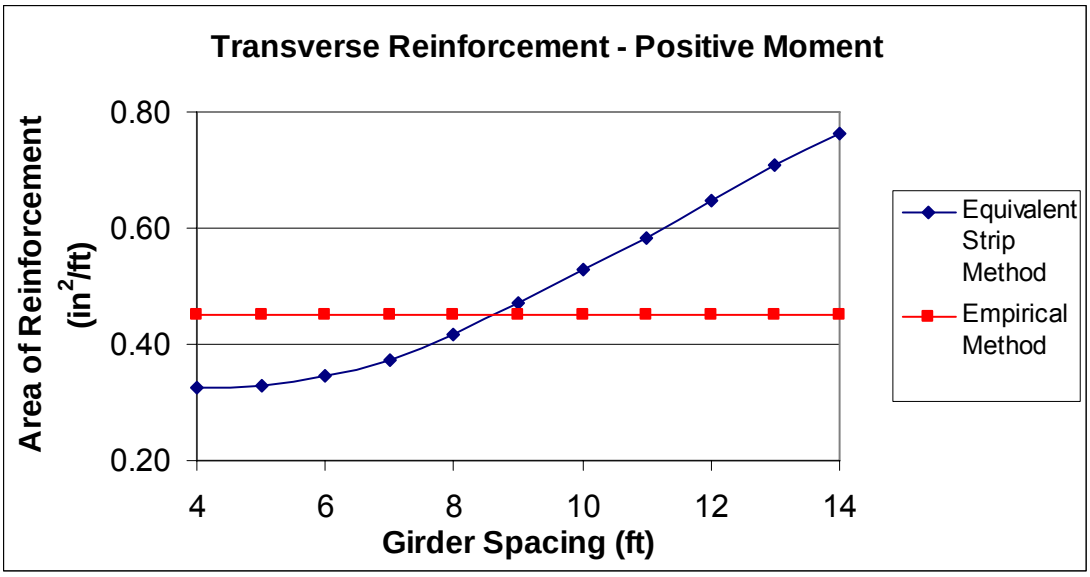

Figure 4-5: Transverse Reinforcement for Positive Moment Regions

The transverse reinforcement in negative moment regions showed a similar trend to that of the transverse reinforcement in positive moment regions. For negative moment regions, the equivalent strip method yielded larger values for the required area of reinforcement for girder spacing larger than approximately 7-feet. These results can be seen in Figure 4-6.

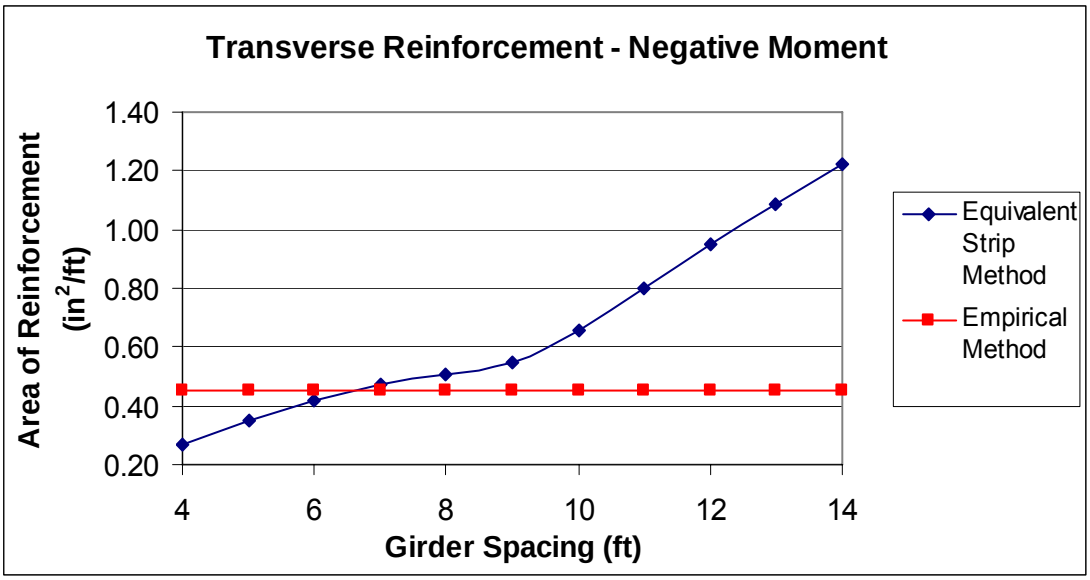

Figure 4-6: Transverse Reinforcement for Negative Moment Regions

The equivalent strip method calculated the bottom layer of longitudinal reinforcement by taking it as a percentage of the longitudinal reinforcement. Therefore, it also increased as the girder spacing increases. The value calculated by the empirical method is less than that calculated by the equivalent strip method for girder spacings greater than 8-feet. Figure 4-7 shows these results.

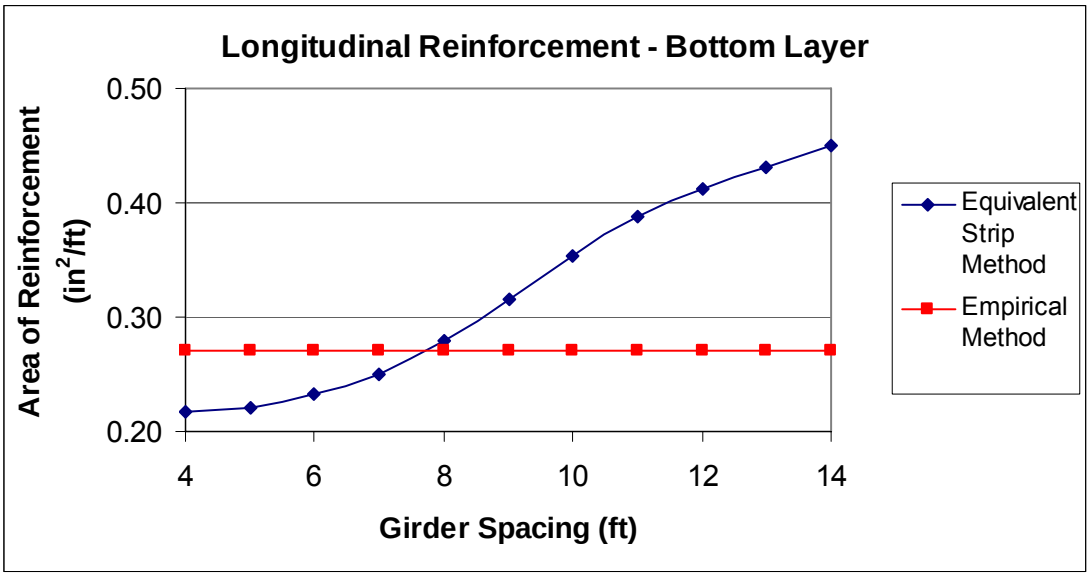

Figure 4-7: Bottom Layer of Longitudinal Reinforcement

The required area for the top layer of longitudinal reinforcement was not compared because the equivalent strip method does not have specific requirements to determine this reinforcement. Many jurisdictions used #4 bars at 12-inches on center, which provide 0.196 in^2/ft of reinforcement which in larger than the empirical method requirements of 0.18 in^2/ft.

The required area of reinforcement determined by the equivalent strip method was calculated with the use of a Microsoft Excel spreadsheet. The values used in Figure 4-4 through 4-6 and the spreadsheet layout used for the calculations can be found in Appendix C.

CHAPTER 5 : MMFX IMPLIMETATION

As part of the study of MMFX, it was used in a bridge deck on a UDOT bridge. The bridge was located in Spanish Fork Canyon near Mile Post 218 and was designated as US-6 (White River Bridge). The bridge is a three span super structure over railroad tracks. The superstructure is made of five steel I girders supporting a reinforced concrete deck. Figures 5.1 and 5.2 show an elevation and underside view of the bridge.

Figure 5.1 Elevation View of MMFX Bridge.

Figure 5.2. Steel Girders of MMFX Deck Bridge

The concrete deck was reinforced with MMFX steel. During placement of the MMFX steel, various construction workers were interviewed. Each worker stated that there was no additional labor involved with placing the MMFX steel in comparison to conventional epoxy coated rebar. In addition, they stated that it was probably a little safer as the rebar was not a slippery, especially when it rained. Figures 5.3 and 5.4 show the MMFX deck steel that was used in this bridge.

Figure 5.3. MMFX Deck Steel

Figure 5.4. Abutment MMFX Deck Steel

CHAPTER 6 : CONCLUSIONS

6.1 MMFX Summary and Conclusions

MMFX Microcomposite Steel is a promising alternative to epoxy-coated rebar due to its enhanced corrosive resistant and structural properties. To date, research has established the enhanced corrosive resistant properties primarily by short-term tests performed in an aqueous corrosive induced environment or with steel embedded in concrete blocks with little data resulting from actual structures. These enhanced corrosive properties are likely due to the increased levels of alloying elements such as chromium (Cr) content.

- The research that has been performed thus far on the corrosive properties of MMFX Microscomposite Steel has demonstrated that it has a critical chloride threshold that is approximately four time higher than that of mild reinforcement (not epoxy-coated rebar).
- Researchers have found that the rate of corrosion of MMFX is smaller (between one-third and two-thirds) of mild reinforcement. Some studies have shown that the corrosive rate increases over time.
- Most stainless steel specimens tested performed better than MMFX Microcomposite Steel, but cost more likely due to their higher chromium contents.
- While many of the rapid tests that have been performed for this research do allow for a quick evaluation that can be used to rate different types of steel, they do not provide a reliable correlation between short-term test results and in-situ results that are required to make accurate life-cycle costs.

Recommendations

- For critical concrete bridge decks that are going to be exposed to large amounts of traffic and salting, UDOT should consider using MMFX steel or some other type clad or stainless steel rebar.
- For Concrete bridge decks that are not exposed to large amounts of traffic and salting, UDOT should consider the continued use of epoxy-coated rebar until more personal experience is gained on the pilot bridge or more long-term data is gained from bridges built with MMFX steel in other states.
- UDOT should monitor the corrosion potential of the pilot bridge.
- UDOT should investigate other types of corrosion resistant reinforcement (i.e. Zn/EC bars).
- UDOT should not use different types of steel for the top and bottom mats until more research is performed to insure that cracking does not occur at the bottom of the deck.

6.2 HPS Summary and Conclusions

Grade HPS 70W is now commercially available because of a research program launched by the FHWA, the U.S. Navy, and AISI. The program goal was to develop high strength steels with improved weldability and increased toughness. High performance steel is the product of this research program. HPS 70W grade steel is now commercially available while HPS 100W grade steel is still under development (FHWA, 2002).

Using HPS in bridges can offer many benefits which can include, reduction in steel weight, reduced number of girder lines, and shallower cross-section which can help with clearance requirements. This study conducted focused on the reduction of the steel girder weight which can in turn decrease the steel cost. Because a reduction in weight does not always represent a decrease in cost, the steel weight and cost were compared. This is because HPS 70W steel is more expensive than grade 50W steel.

To be able to determine where and when HPS is advantageous, three design alternatives were compared. These design alternatives used 50W steel, HPS 70W steel, and a hybrid combination of the previous two for the steel girders. The designs were then

compared at several different span lengths for one and two span bridges. When comparing the weight of the steel girders the following was observed:

- Single Span: Both HPS designs(HPS 70W and hybrid sections) showed small weight reductions in comparision to the 50W steel.
- Two-Span: The hybrid design alternative had the lightest steel weight for span lengths up to 100-feet .
- Two-Span: the homogeneous HPS 70W design had the lowest steel weights for spans greater than 100-ft, which resulted in an average weight reduction of approximatley 42%.

The cost of the three alternatives was also compared and resulted in the following:

- Single Span: Homgeneous HPS 70W design was the most expensive alternative for all span lengths
- Single Span: Hybrid designs reduced the price for spans lengths up to 150-feet, with a maximum price reduction of 27% in comparision to the 50W section.
- Two-Span: Hybrid design had the lowest cost for all span lengths up to 200-feet, with a maximum price reduction of 37% in comparison to the 50W section.

This study has showed that the steel weight and cost can be reduced by using HPS. Although, the use of HPS does not always result in a weight or cost reduction. It is also observed that in general more advantages were seen when using HPS in two-span continuous bridges than in single span bridges.

The two deck design methods described in the AASHTO- LRFD Bridge Design Specifications (2004) was also compared in this study. These methods include the Empirical Design Method and the Equivalent Strip Method. The two methods yield different required areas of deck steel. The methods compared the required amount of deck steel for various girder spacings. The girder spacings were varied from 4 to 14 feet. The Equivalent Strip Method required a larger area of deck steel for the following cases:

- Positive moment transverse reinforcement for girder spacings larger than 9-feet.
- Negative moment transverse reinforcement for girder spacings larger than 7-feet.
- Bottom layer of longitudinal reinforcement for girder spacings larger than 8-feet.

In general, for girder spacings larger than 9-feet, the Empirical Design Method requires the least amount of deck reinforcement. For girder spacings less than 7-feet, the Equivalent Strip Method requires the least amount of deck steel.

REFERENCES

Ahlborn, T., and Denhartigh, T. (2002). "A Comparative Bond Study of MMFX Reinforcing Steel in Concrete." Michigan Technology University Center for Structural Durability, Houghton, Michigan.

Ansley, M. (2002). "Investigation into the structural Performance of MMFX Reinforcing." Florida Department of Transportation Structures Research Center.

Barker, M., and Schrage, S., (2000). "High Performance Steel: Design and Cost Comparisons." Bridge Crossings, NSBA, 16(1).

Clemena, G.G and Virmani, Y. P. (2003). "Comparison of the Corrosion Resistance of Some New Metallic Reinforcing Bars in Concrete Blocks Exposed to Chloride Ions." Virginia Transportation Research Council, Charlottesville, Virginia, *VTCR 04-R7*.

Concrete Reinforcing Steel Institute (CRSI). (1998). "Epoxy-Coated Rebar Delivers Cost-Effective Value." Schamburg, Illinois.

Cooper, J., Lane, S., Munley, E., Simon, M., and Wright, B., (1998). "Focus on High-Performance." Better Roads

El-Hacha, R. and Rizkalla, S. H. (2002). "Fundamental Material Properties of MMFX Steel Rebars." Constructed Facilities Laboratory (CFL), NC State University, Raleigh, North Carolina.

Federal Highway Administration (FHWA), (2002). "High Performance Steel Designers' Guide." U.S. Department of Transportation.

Federal Highway Administration (FHWA), (2002). "A High Performance Steel Scorecard." Focus Accelerating Infrastructure Innovations.

Hartt, W., Lysogorski, D. and Leroux, V. (2004). "Characterization of Corrosion Resistant Reinforcement by Accelerated Testing." CBC Conference Paper. pp. 12.

Hartt, W. H., Rodney G. Powers, R. G., Leroux, V., and Lysogorski. D. K. (2004). "A Critical Literature Review of High-Performance Corrosion Reinforcements in Concrete Bridge Applications." Federal Highway Administration, FHWA-HRT-04-093, McLean, VA.

Hill, C., Chiaw, C. C. and Harik, I. E. (2003). "Reinforcement Alternatives for Concrete Bridge Decks." Kentucky Transportation Center, *KTC-03-19/SPR-215-00-1F*.

Huff, T., Pate, W., and Wasserman, E., (2005). "The Evolution of Best Practices with High Performance Steel for Bridges." *2003 ECI Conference on Advanced Materials for Construction of Bridges, Buildings, and Other Structures III.*" Davos, Switzerland.

Jolley, M. J. (2003). "Evaluation of Corrosion-Resistant Steel Reinforcement." Iowa State University.

Latiolait, J. (2002). "Report of A615 Equivalent Reinforcing Steel." Smith-Emery Laboratories, Los Angeles, CA, *Project No. 31227-1.*

Malhas, F. A. (2002). "Preliminary Experimental Investigation of the Flexural Behavior of Reinforced Concrete Beams using MMFX Steel." Final Report for MMFX Technologies Corporation, Irvine, CA.

Ooyen, Kristi., (2002). "HPS Success." AISC Modern Steel Construction, 9(1).

Peterfreund, S. W. (2003). "Development Length of Micro-Composite (MMFX) Steel Reinforcing Bars used in Bridge Deck Applications." Senior Honors Project, Department of Civil and Environmental Engineering, University of Massachusetts, Amherst.

Pfeifer, D.W., (2000). "High Performance Concrete and Reinforcing Steel with a 100-Year Service Life." *PCI Journal*, V. 45, No. 3, May-June, pp. 46-54.

Povov, B.N., Haran,, B., and Colon, H. (2002). "Corrosion Evaluation of MMFX Reinforcing Steel." Preliminary Report submitted to MMFX Corporation of America, Charlotte, North Carolina.

Stephan, B., Restrepo, J. and Seible, F. (2003). "Seismic Behavior of Bridge Columns Built Incorporating MMFX Steel." University of California, San Diego, *Report No. SSRP-2003/09*.

Trejo, D. and Pillai, R. G. (2003). "Accelerated Chloride Threshold Testing: Part 1-ASTM A 615 and A 706 Reinforcement." *ACI Materials Journal*, 100(6), November-December, 519-527.

Trejo, D. and Pillai, R. G. (2004). "Accelerated Chloride Threshold Testing-Part II: Corrosion-Resistant Reinforcement." *ACI Materials Journal*, 101(1), January-February, 57-64.

Vijay, P. V., GangaRao, H. V. S., and Woraphot, P. (2002). "Bending Behavior of Concrete Beams Reinforced with MMFX Steel Bars." The Construction Facilities Center, West Virginia University, Morgantown, WV.

Virginia Transportation Research Council. (2003). "Testing of Selected Metallic Reinforcing Bars for Extending the Service Life of Future Concrete Bridges." VTRC 03-R7RB, June 2003.

Virmani, Y.P. (1997). "Epoxy-Coated Rebars in Bridge Decks." FHWA Technical Note on Corrosion Protection Systems, Structures Division, Office of Engineering Research and Development.

Yunovich, M., Thompson, N. G., Balvanyos, T. and Lave, L. (2001), "Corrosion Costs and Preventative Strategies in the United States." Report by CC Technologies to Federal Highway Administration, *Report FHWA-RD-01-156*.

Zia, P., Bremner, T.W., Malhotra, V.M., Schupack, M., and Tourney, P.G., "High Corrosion Resistance MMFX Microcomposite Reinforcing Steel." MMFX Technologies Corporation, Irvine, California.

APPENDIX A

Weight Comparison

1 - SPAN					
Span	Material	Weight per Girder (lbs.)	Failure Mode	% Weight Decrease	Comments
50	50W	4500	Strength IV		W-section
50	70W	4500	Strength IV	0.00%	W-section
50	HPS 70W/ 50W	3875.97	Strength IV	13.87%	Plate Girder
75	50W	11175	Service II		W-section
75	70W	10125	Strength IV	9.40%	W-section
75	HPS 70W/ 50W	8804.69	deflection	21.21%	Plate Girder
100	50W	23000	Service II/ Strength I		W-section
100	70W	21500	deflection	6.52%	W-section
100	HPS 70W/ 50W	15184.9	deflection	33.98%	Plate Girder
125	50W	41875	Strength & Deflection		W-section
125	70W	41875	deflection	0.00%	W-section
125	HPS 70W/ 50W	32273.22	deflection	22.93%	Plate Girder
150	50W	55451.67	stress/def		All Plate Girders
150	70W	50036.15	deflection	9.77%	weight taken out of web
150	HPS 70W/ 50W	50036.15	deflection	9.77%	Plate Girder
175	50W	86250.21	stress		Plate Girder
175	70W	78806.63	deflection	8.63%	weight taken out of web
175	HPS 70W/ 50W	78806.63	deflection	8.63%	Plate Girder
200	50W	129530.14	deflection		Plate Girder
200	70W	117048.75	deflection	9.64%	Plate Girder
200	HPS 70W/ 50W	117048.75	deflection	9.64%	Plate Girder

2 - SPAN					
Span	Material	Weight per Girder (lbs.)	Failure Mode	% Weight Decrease	Comments
50-50	50W	8000	Strength I		W-Section
50-50	70W	8000	Strength I	0.00%	W-Section
50-50	HPS 70W/ 50W	6486.55	Strength I	18.92%	Plate Girder
75-75	50W	17250	Strength I		W-Section
75-75	70W	14925	Strength I	13.48%	W-Section
75-75	HPS 70W/ 50W	12696.61	Strength I	26.40%	Plate Girder
100-100	50W	39700	Strength I		W-Section
100-100	70W	29000	Strength I	26.95%	W-Section
100-100	HPS 70W/ 50W	22330.73	Strength I	43.75%	Plate Girder
125-125	50W	54869.79	Strength I		Plate Girder
125-125	70W	40301.65	Strength I	26.55%	Plate Girder
125-125	HPS 70W/ 50W	41471.35	Strength I	24.42%	Plate Girder
150-150	50W	86005.21	Strength I		Plate Girder
150-150	70W	49280.73	Strength I	42.70%	Plate Girder
150-150	HPS 70W/ 50W	50454.69	Strength I	41.34%	Plate Girder
175-175	50W	135473.09	Strength I		Plate Girder
175-175	70W	76132.9	Strength I	43.80%	Plate Girder
175-175	HPS 70W/ 50W	78604.17	Strength I	41.98%	Plate Girder
200-200	50W	179326.39	Strength I		Plate Girder
200-200	70W	97795.84	Strength I	45.46%	Plate Girder
200-200	HPS 70W/ 50W	103104.17	Strength I	42.50%	Plate Girder

APPENDIX B

Equivalent Strip Method Calculation Spreadsheet

Section

S4.1 **Bridge Dimensions**

		Units
Girder Spacing (ft)	8.00	ft
Top Flange Width (in)	14	in
Slab. Conc. Comp Strength (ksi)	4	ksi
Concrete Density (pcf)	150	pcf
Future Wearing Surface (psf)	30	psf
Deck Thickness (in)	7.5	in
Integral Wearing Surface (in)	0.5	in

S4.1 **Reinforcement Properties**

		Units
Reinforcement Yield Strength (ksi)	60	ksi
Top Cover (in)	2.5	in
Bottom Cover (in)	1	in
Rebar Diameter	0.625	in

S4.3.1 **Load Factors (S3.4.1)**

Max Slab and Parapet	1.25
Future Wearing Surface	1.5

Dead Loads & Moments

Deck	100.00	psf
FWS	30.00	psf
Deck Moment per unit width	0.64	k-ft/ft
FWS moment per unit width	0.19	k-ft/ft
Fact. Deck Moment per unit width	0.80	k-ft/ft
Fact. FWS Moment per unit width	0.29	k-ft/ft

S4.3.5

Girder Center to Neg. Mom. Section	4.67	in

S4.3.2 **Live Load Factors**

Dynamic Load Allowance	0.33
Strength Load Factor	1.75
Multiple Presence Factors	
Single	1.2
Two Lane	1.0
Three Lane	0.85
Resistance Factors	
Strength Limit State	0.9
Extreme Limit State	1.0

S4.3.3 Positive Moment - Transverse Reinforcement

Positive LL Moment per unit width	5.69	k-ft/ft
Max. Fact. LL Moment per unit width	9.96	k-ft/ft
Post. DL + LL Moment (Strength I)	11.05	k-ft/ft

Required Area of Steel

de	6.19	in
k'	0.32	k/in^2
ρ	0.01	
Required Area of Steel	0.035	in^2/in

Reinforcement Options - Bar Size & Spacing

Bars	Spacing	Units
#4	5.65	in
#5	8.82	in
#6	12.70	in
#7	17.29	in
#8	22.58	in

Positive Moment - Strength Limit State Use:

#6 Bar	**8.82**	in
area of bar	**0.31**	in^2

OK

Max. Reinforcement Check

Reinf. Tensile Force	18.41	k
a	0.61	in
β_1	0.85	
c	0.72	in
c/de < 0.42	0.12	

OK

S4.3.4 Check Cracking (S5.7.3.4) - Positive Moment Trans. Steel

$$f_{sa} = \frac{Z}{(d_c A)^{\frac{1}{3}}} \le 0.6 f_y$$

d_c	1.31	in
A	23.15	in^2
Z (crack control parameter - Extreme)	130	k/in
fsa calculated	41.66	ksi
Fsa (allowed)	**36.00**	ksi

OK

Stresses under service loads

n (modular ratio)	8	
Dead Load Serve Moment	0.83	k-ft/ft

Live Load Service Moment	5.69	k-ft/ft
DL + LL Service Positive Moment	6.52	k-ft/ft
A- transformed steel area	2.45	in^2
y	1.60	in
I transformed	60.78	in^4
x (dist from neutral axis to steel)	4.59	in
Fs (stress in steel) < Fsa	**34.75**	ksi

OK

S4.3.6 Negative Moment - Transverse Reinforcement

Unfactored Neg. LL Moment	5.65	k-ft/ft
Factored Neg LL Moment	9.89	k-ft/ft
Deck Weight Moment	0.80	k-ft/ft
FWS Moment	0.29	k-ft/ft
Neg. DL + LL Moment (Strength I)	10.98	k-ft/ft
d (comp face to tension reinf)	5.19	in
k'	0.45	k/in^2
ρ	0.01	
Required Area of Steel	0.04	in^2/in

Reinforcement Options - Bar Size & Spacing

Bars	Spacing	Units
#4	4.65	in
#5	7.27	in
#6	10.47	in
#7	14.25	in
#8	18.61	in

Negative Moment - Strength Limit State Use:

#6 Bar	**7.26**	in
area of bar	**0.31**	in^2

OK

S4.3.7 Check Cracking (S5.7.3.4) - Negative Moment Trans. Steel

$$f_{sa} = \frac{Z}{(d_c A)^{\frac{1}{3}}} \le 0.6 f_y$$

d_c	2.31	in
A	33.58	in^2
Z (crack control parameter -Extreme)	130.00	k/in
fsa calculated	30.47	ksi
Fsa (allowed)	**30.47**	ksi

Stress under Service Loads

n (modular ratio)	8.00	
Dead Load Serve Moment	0.83	k-ft/ft

Live Load Service Moment	5.65	k-ft/ft	
DL + LL Service Positive Moment	6.48	k-ft/ft	
A- transformed steel area	2.45	in^2	
y	1.57	in	
I transformed	44.78	in^4	
x (dist from neutral axis to steel)	3.62	in	
Fs (stress in steel) < Fsa	**30.45**	ksi	**OK**

S4.3.8 Longitudinal Reinforcement

$$\%\ Long.\ \text{Re inf}\ orcement = \frac{220}{S} \le 67\%$$

S	8.00	ft
Percentage (calculated	0.78	%
Percentage (use)	0.67	%
Transverse Reinforcement	0.42	in^2/ft
Longitudinal Reinforcement	0.28	in^2/ft

Reinforcement Options - Bar Size & Spacing

Bars	Spacing	Units
#4	8.43	in
#5	13.16	in
#6	18.96	in
#7	25.80	in
#8	33.70	in

Bottom Longitudinal Reinforcement

#5 Bar	**13.16**	in	
area of bar	**0.31**	in^2	**OK**

Top Longitudinal Reinforcement

#4 Bar (common)	**12**	in	
area of bar	**0.1963**	in^2	**OK**

S4.3.9 Shrinkage and Temperature Reinforcement

Ag	90	in^2	
As required per surface	0.0825	in^2/ft	**OK**

Legend

Pink	Dimensions and Factors
Blue	Dependent on Girder Spacing
Orange	Pick from Reinforcement sizes and spacings

APPENDIX C

Transverse Reinforcement - Positive Moment

Girder Spacing (ft)	Equivalent Strip Method - Area of Reinforcement (in^2/ft)	Empirical Method - Area of Reinforcement (in^2/ft)
4	0.32494	0.45
5	0.32871	0.45
6	0.34732	0.45
7	0.37414	0.45
8	0.41741	0.45
9	0.47139	0.45
10	0.52744	0.45
11	0.58345	0.45
12	0.64810	0.45
13	0.70686	0.45
14	0.76390	0.45

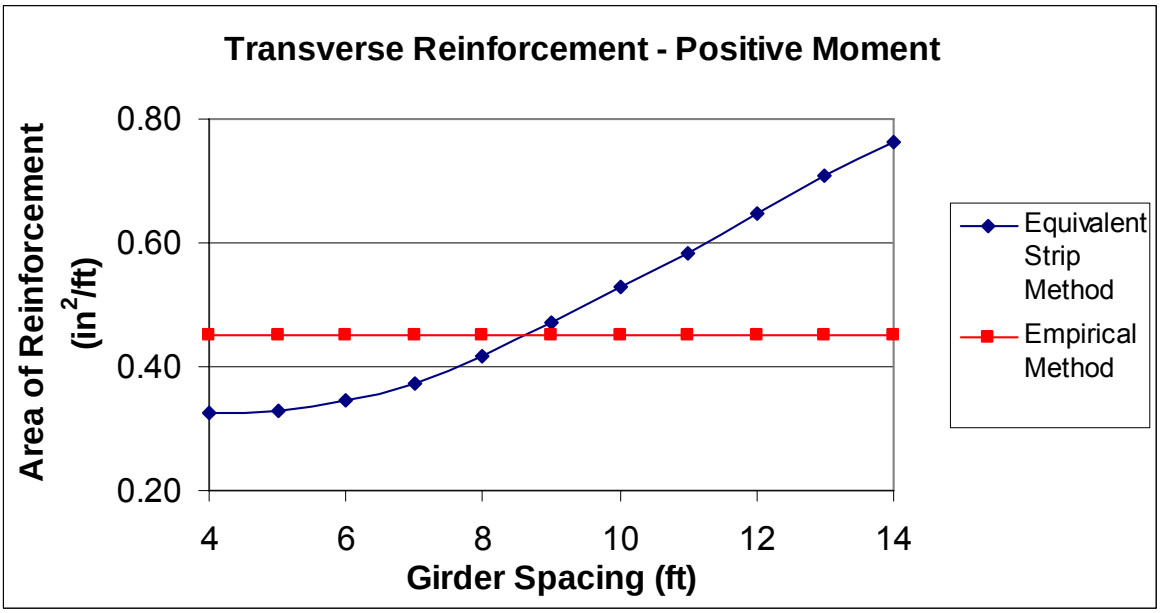

Transverse Reinforcement - Negative Moment

Girder Spacing (ft)	Equivalent Strip Method - Area of Reinforcement (in^2/ft)	Empirical Method - Area of Reinforcement (in^2/ft)
4	0.26582	0.45
5	0.34896	0.45
6	0.41599	0.45
7	0.47443	0.45
8	0.50710	0.45
9	0.54949	0.45
10	0.65860	0.45
11	0.79860	0.45
12	0.95008	0.45
13	1.08636	0.45
14	1.22153	0.45

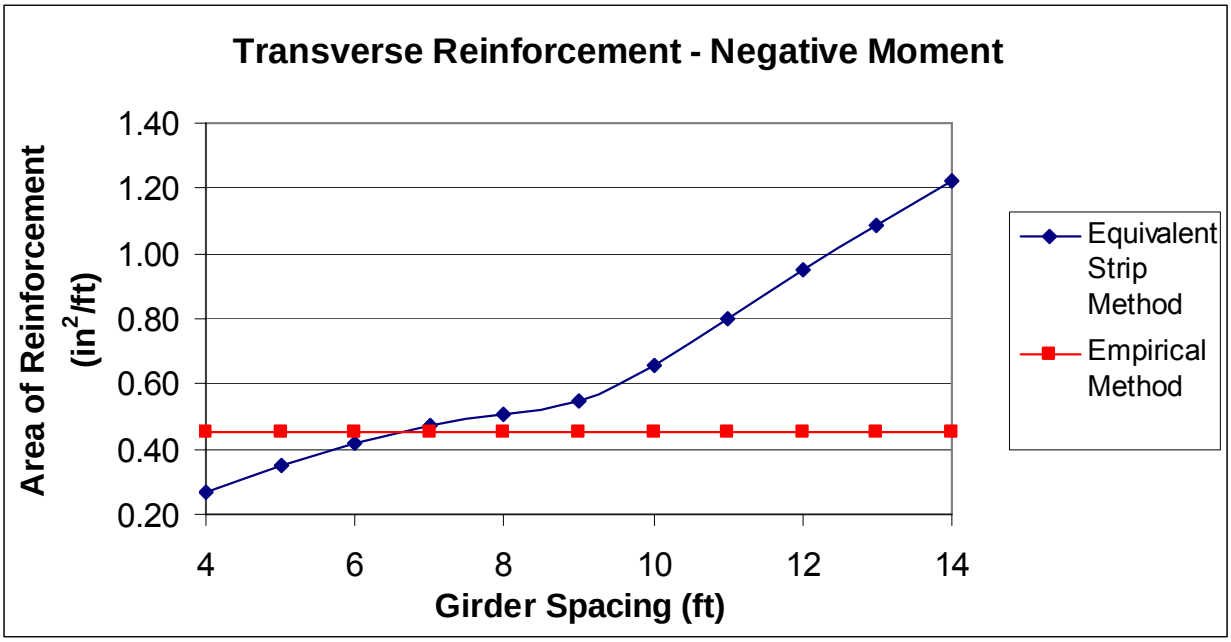

Longitudinal Reinforcement - Bottom Layer		
Girder Spacing (ft)	Equivalent Strip Method - Area of Reinforcement (in^2/ft)	Empirical Method - Area of Reinforcement (in^2/ft)
4	0.21786	0.27
5	0.22033	0.27
6	0.23287	0.27
7	0.25078	0.27
8	0.27994	0.27
9	0.31595	0.27
10	0.35355	0.27
11	0.38738	0.27
12	0.41208	0.27
13	0.43138	0.27
14	0.44927	0.27